UNIVERSITA' DEGLI STUDI DI PARMA

Dottorato di ricerca in Fisiopatologia Sistemica

Ciclo XXIII

EARLY TREATMENT WITH A NATURAL ANTIOXIDANT POLYPHENOLIC COMPOUND (RESVERATROL: TRANS-3,5,4'-TRIHYDROXYSTILBENE): A NEW ADJUVANT THERAPEUTIC APPROACH FOR PREVENTING DIABETIC CARDIOMYOPATHY, IN EXPERIMENTAL TYPE-1 DIABETES

Coordinatore:
Chiar.mo Prof. Enrico Maria Silini

Tutor:
Chiar.ma Prof. ssa Donatella Stilli

Dottorando:
Dott.ssa Francesca Delucchi

“Io abiterò il mio nome”

Saint-John Perse – Esilio

Abstract

Emerging evidence suggests that both adult cardiac cell and the cardiac stem/progenitor cell (CSPC) compartments are involved in the patho-physiology of diabetic cardiomyopathy (DCM). We evaluated whether early administration of Resveratrol, a natural antioxidant polyphenolic compound, in addition to improving cardiomyocyte function, exerts a protective role on (i) the progenitor cell pool, and (ii) the myocardial environment and its impact on CSPCs, positively interfering with the onset of DCM phenotype.

Adult Wistar rats (n=128) with streptozotocin-induced type-1 diabetes were either untreated (D group; n=54) or subjected to administration of trans-Resveratrol (i.p. injection: 2.5 mg/Kg/day; DR group; n=64). Twenty-five rats constituted the control group (C). After 1, 3 or 8 weeks of hyperglycemia, we evaluated cardiac hemodynamic performance, and cardiomyocyte contractile properties and intracellular calcium dynamics. Myocardial remodeling and tissue inflammation were also assessed by morphometry, immunohistochemistry and immunoblotting. Eventually, the impact of the diabetic “milieu” on CSPC turnover was analyzed in co-cultures of healthy CSPCs and cardiomyocytes isolated from D and DR diabetic hearts.

In untreated animals, cardiac function was maintained during the first 3 weeks of hyperglycemia, although a definite ventricular remodeling was already present, mainly characterized by a marked loss of CSPCs and adult cardiac cells. Relevant signs of ventricular dysfunction appeared after 8 weeks of diabetes, and included: 1) a significant reduction in ±dP/dt in comparison with C group, 2) a prolongation of isovolumic contraction/relaxation times, 3) an impaired contraction of isolated cardiomyocytes associated with altered intracellular calcium dynamics. Resveratrol administration reduced atrial CSPC loss, succeeded in preserving the functional abilities of CSPCs and mature cardiac cells, improved cardiac environment by reducing inflammatory state and decreased unfavorable ventricular remodeling of the diabetic heart, leading to a marked recovery of ventricular function. These findings indicate that RSV can constitute an adjuvant therapeutic option in DCM prevention and treatment.

CONTENTS

Introduction

Diabetic Cardiomyopathy

Cardiovascular disease represents the major cause of morbidity and mortality in diabetic patients [1]. Accumulating data from experimental, pathological, epidemiological, and clinical studies have shown that diabetes mellitus results in cardiac functional and structural changes which develop independently of hypertension, coronary artery disease, or any other known cardiac diseases, supporting the existence of a specific diabetic cardiomyopathy (DCM) [2,3]. The concept of DCM was first introduced by Rubler et al. [4] in 1972, who reported the autopsy data from four patients with diabetic renal microangiopathy and dilated left ventricles in the absence of other common causes.

By definition, diabetic cardiomyopathy is a distinct primary disease process which occurs independently of common comorbidities and secondary to a metabolic insult, resulting in structural and functional abnormalities of the myocardium leading to heart failure (HF).

Despite the potential importance of this disease entity, the complex and multifactorial nature of the cellular and molecular perturbation that predispose to altered myocardial structure and function remains incompletely understood.

Pathophysiologic mechanisms of diabetic cardiomyopathy

The pathogenesis of diabetic cardiomyopathy is multifactorial (Fig. 1). Several hypotheses have been proposed, including autonomic dysfunction, metabolic derangements, abnormalities in Ca^{2+} homeostasis, alteration in structural protein, and interstitial fibrosis. The variety of proposed mechanisms advanced for the pathogenesis of diabetic cardiomyopathy likely reflects the complex nature of this disease.

The metabolic environment, characterized by hyperglycemia, hyperinsulinemia, and hyperlipidemia (usually in the form of increased triglycerides and non-esterified fatty acids – NEFAs), in which diabetic heart functions, certainly triggers a substantial amount of cellular, structural and functional alterations progressively leading to DCM phenotype.

In particular, hyperglicemia is considered to be a central driver in the pathophysiology of diabetic cardiomyopathy, in both type-1 and type-2 diabetes.

Type 1 diabetes differs principally from type 2 diabetes in that it is unaccompanied by a period of hyperinsulinemia and is characterized by early – as opposed to late – onset of hyperglycemia.

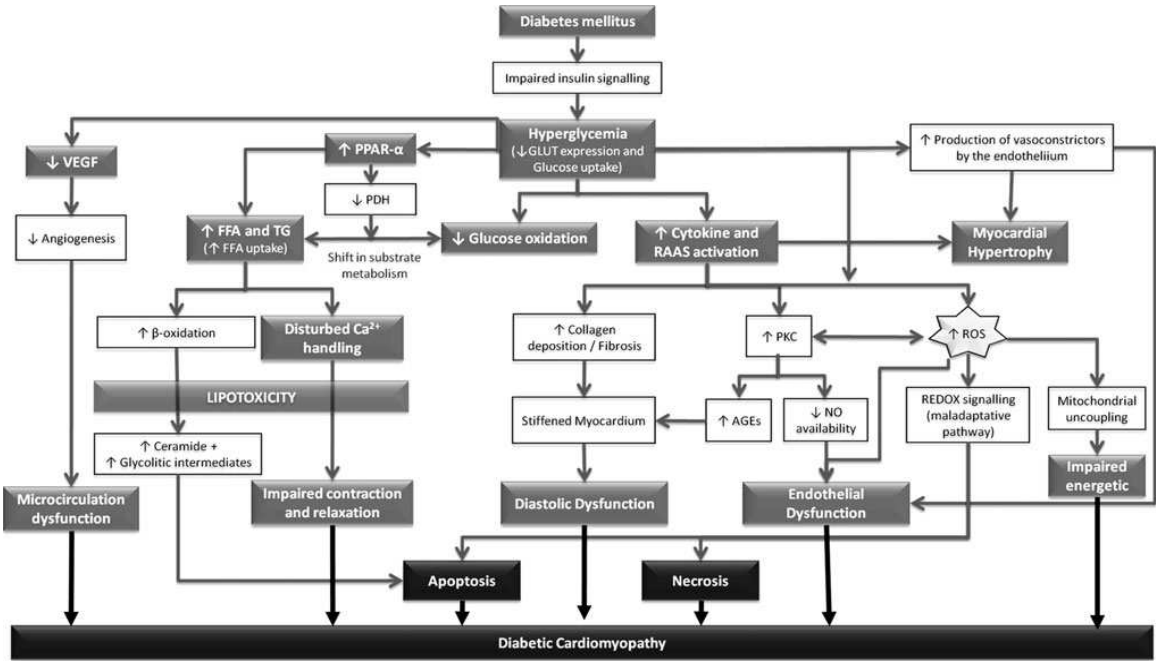

Figure 1. Pathophysiologic mechanisms of diabetic cardiomyopathy. AGEs advanced glycation end-products, FFA free fatty acids, GLUT glucose transporter, NO nitric oxide, PDH pyruvate dehydrogenase, PKC protein kinase C, PPAR-a peroxisome proliferator–activated receptor-a, ROS reactive oxygen species, TG triglycerides, VEGF vascular endothelial growth factor.

Hyperglicemia

Hyperglicemia represents one of the most important triggers of metabolic changes in diabetes [5]. In the absence of diabetes, approximately equivalent proportions of energy required for cardiac contractility come from glucose metabolism and free fatty acids (FFA), whereas in diabetes, myocardial glucose use is significantly reduced, with a shift in energy production toward FFA β-oxidation [6].

The reduction in glucose use in the diabetic myocardium results from depleted glucose transporter proteins, glucose transporter-1 (GLUT-1) and GLUT-4. In addition, a second mechanism of reduced glucose oxidation is via the inhibitory effect of fatty acid oxidation on pyruvate dehydrogenase complex due to high circulating free fatty acids, this induces an impairment in the myocardial energy production and leads to the accumulation of glycolitic intermediates and ceramide, enhancing apoptosis [7,8]. Also, peroxisome proliferators-activator receptor-α (PPAR-α)-enhanced activity in diabetes mellitus (DM) increases the expression of pyruvate dehydrogenase kinase 4 and other genes involved in the regulation of cellular FFA uptake and β-oxidation and also reduces glucose oxidation.

Furthermore, high levels of FFA are believed to be one of the major contributing factor in the pathogenesis of diabetes. Elevation of circulating FFAs is caused by enhanced adipose tissue lipolysis, and increased tissue FFAs are caused by the hydrolysis of augmented myocardial triglyceride stores. They enhance peripheral insuline resistance and trigger cell death. Moreover, in addition to the FFA induced inhibition of glucose oxidation, high circulating and cellular FFA levels may result in intracellular accumulation of potentially toxic intermediates of FFA (lipotoxicity), besides the abnormally high oxygen requirements during FFA metabolism. All these changes lead to severe morphological changes [9, 10, 11] and impaired myocardial performance [12, 13, 14].

Oxidative stress: reactive oxygen species (ROS)

Under physiological conditions, reactive oxygen species (ROS), such as superoxide radical, hydroxyl radical, and hydrogen peroxide (H_2O_2) are continuously produced in many cells, but ROS levels are regulated by a number of enzymes and physiological antioxidants, such as superoxide dismutase, glutathione peroxidase, catalase, and thioredoxin.

However, when the production of ROS outweighs their degradation by antioxidant defences, oxidative stress will develop and impose a harmful effect on the functional integrity of biological tissues.

Large experimental and clinical studies have shown that the generation of ROS is increased in both types of diabetes and that the onset of diabetes and its complications, including diabetic cardiomyopathy, are associated with oxidative stress [15, 16]. It has been postulated that hyperglycemia may produce ROS through the formation of advanced glycation end products (AGEs) [17, 18] and altered polyol pathway activity [19], and through the activation of NADPH oxidase *via* protein kinase C (PKC) [20]. The increase in ROS, closely related with mitochondrial damage, causes cardiac dysfunction by direct damage to proteins and DNA as well as by promoting apoptosis [21, 22], abnormalities in calcium homeostasis and endothelial dysfunction [23, 24]. Cell death is an important determinant of cardiac remodeling because it causes a loss of contractile units, compensatory hypertrophy of myocardial cells and reparative fibrosis [25].

Even if it is well documented that the increase in oxidative stress plays an important role in the development of diabetic cardiomyopathy [26], the precise mechanism(s) by which ROS accumulation leads to compromised heart function and the effect of antioxidant therapy in diabetic subjects is largely unknown, although experimental data suggest that regimes targeting reduction of ROS or increasing antioxidant activity potentially represent novel therapeutic modalities for diabetic cardiomyopathy.

In Figure 2 are summarized the interactions between the myocardial and vascular changes present in diabetic hearts and their contribution to diabetic cardiomyopathy and heart failure

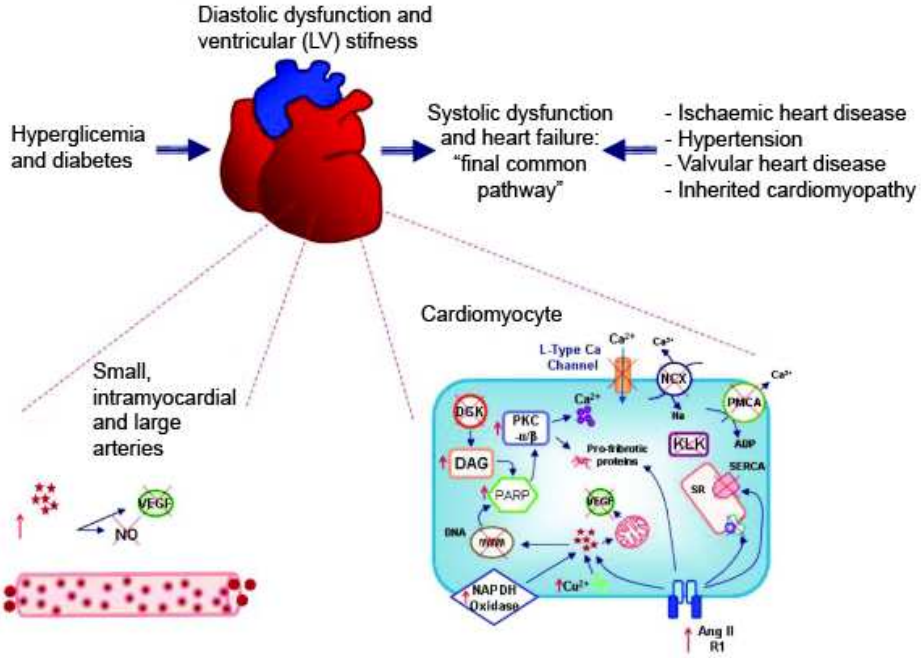

Figure 2. Summary of the interactions between the myocardial and vascular changes present in diabetic hearts and their contribution to diabetic cardiomyopathy and heart failure**.**

Stem cell involvement

Emerging evidence suggests that, not only adult cardiac cells, but also cardiac stem/progenitor cell (CSPC) compartments are involved in the pathophysiology of DCM. It has been shown that several sub-populations of CSPCs reside within the adult heart and possess the ability to differentiate into all constituent cells of cardiac tissue including cardiomyocytes, vascular smooth muscle, endothelial cells and fibroblasts [27, 28].

In early phases of diabetes, the activation of CSPCs associated with proliferation of functionally competent and properly integrated myocytes was shown to represent a compensatory mechanism to counteract cell loss and to preserve cardiac electromechanical performance [29]. However, later phases of diabetes are characterized by progressive CSPCs damage and exhaustion associated with the loss of the physiological balance between cell death and regeneration, leading to overt ventricular dysfunction [30, 31] (Fig. 3).

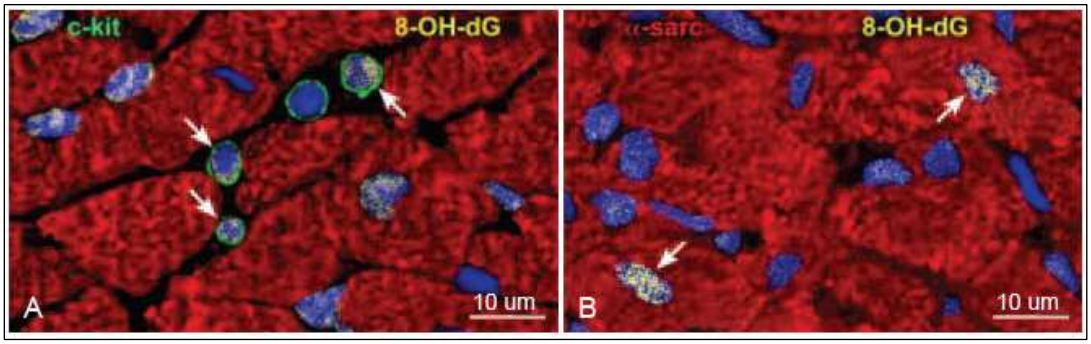

Figure 3. Oxidative DNA damage in CSPCs (A) and myocytes (B) with high nuclear content of 8-hydroxydeoxyguanosine (8-OH-dG).

Antioxidant treatment

Strategies aimed at preserving both parenchymal cells and the pool of progenitor cells responsible for tissue homeostasis may represent an innovative approach for DCM prevention and treatment.

As previously described high levels of oxidative stress trigger cellular damage pathways and are critically involved in cardiac stem/progenitor and parenchimal cell loss [32, 33].

It follows that therapies able to reduce ROS and to enhance ROS scavenging systems should have a promising therapeutic efficacy.

Resveratrol (RSV)

Resveratrol (3,5,4′-trihydroxystilbene) is a non-flavonoid polyphenolic compound abundant in grapes, peanuts and other foods that are commonly consumed as part of human diet (Fig. 4). The compound was first isolated from the root of Polygonum cuspidatum, a plant used in traditional Chinese and Japanese medicine [34]. Polyphenols accumulate in plants in response to exogenous stress factors such as injury, fungal infections or UV irradiation [35]. Humans have been exposed to dietary polyphenols for millions of years, and have developed tolerance to this group of plant defense compounds [36, 37].

Starting in the 1990s and continuing to date, scientific studies have reported that RSV has a broad range of desiderable biological actions, in particular a primary impetus for research on RSV was initiated from the paradoxical observation that a low incidence of cardiovascular diseases may co-exist with a high-fat diet intake and moderate consumption of red wine [38, 39], a phenomenon known as the French Paradox [40].

Besides its antioxidant, anti-apoptotic/anti-inflammatory effects, RSV was shown to exert several other cardioprotective actions, in both ischemic and diabetic rat heart [41, 42, 43]. In experimental models of diabetes, it has been reported that RSV administration reduces reactive oxygen species [44] and the incidence of cardiomyocyte death [45, 46], and improves cardiac function by enhancing the expression of sarcoplasmic calcium ATPase (SERCA2a) in cardiomyocytes, through the activation of deacetylase silent information regulator 2/sirtuin 1 (SIRT1) [47].

Recent data also indicate that RSV may exert beneficial effects on cultured human circulating endothelial progenitor cells, at least in part mediated by inhibited p38-phosphorylation and enhanced NO levels [48]. Finally, in rat models of myocardial infarction subjected to stem-cell regenerative therapy, pre-treatment with RSV was shown to enhance stem cell survival and proliferation [49].

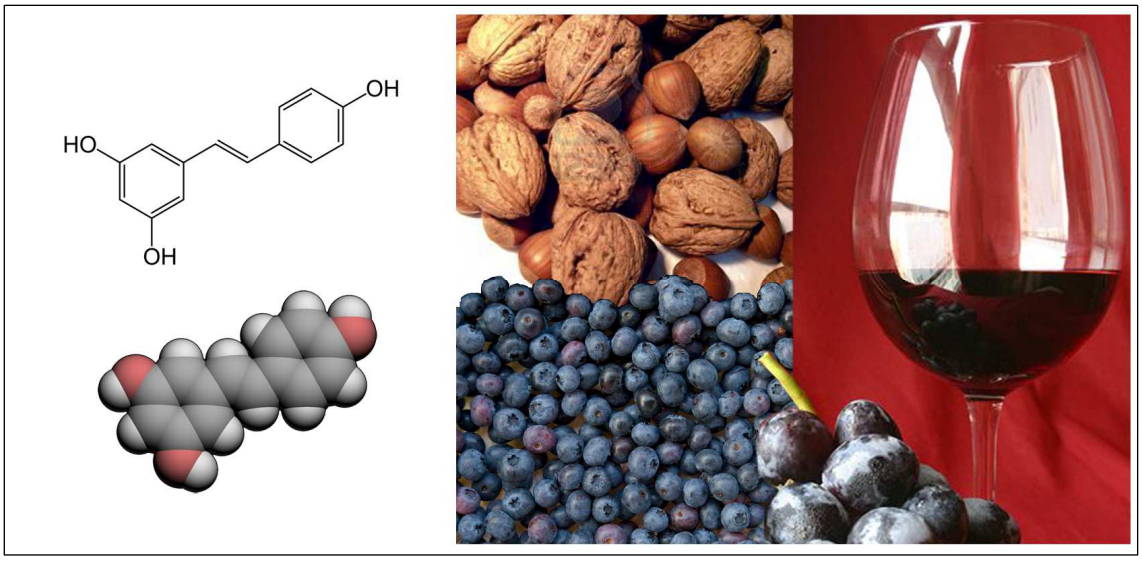

Figure 4. RSV molecule and food sources.

Aim of the thesis

Although RSV holds great promise in the treatment of DCM by regulating several target molecules that protect the myocardium and prevent morpho-functional ventricular remodeling, the potential RSV-induced improvement in the number and function of adult CSPCs in diabetic hearts remains to be explored.

In the present study we specifically addressed this issue in a rat model of STZ-induced diabetes, one of the most commonly used experimental model of type 1 diabetes particularly useful in examining the effects of hyperglycemia without hyperinsulinemia, associated with modest hypertriglyceridemia and ketosis [50].

Following an approach from intact animal to tissue-cellular-molecular level, we tested the hypothesis that early administration of RSV can prevent the onset and development of DCM.

Thus, at different times after the induction of hyperglycemia, we evaluated the potential protective role of RSV on (i) the progenitor cell compartment, positively interfering with the onset and development of DCM phenotype, (ii) the myocardial environment and its impact on CSPC survival and functional properties, (iii) the changes in the relative expression of cardiac actin isoforms usually associated with the progression of myocardial damage [51]. The functional counterpart of the above processes was also evaluated, in terms of hemodynamics and cardiomyocyte contractile properties.

Materials and Methods

The investigation was approved by the Veterinary Animal Care and Use Committee of the University of Parma-Italy and conforms to the National Ethical Guidelines of the Italian Ministry of Health (Permit number: 41/2009-B) and the Guide for the Care and Use of Laboratory Animals (National Institute of Health, Bethesda, MD,USA, revised 1996). All surgery was performed under ketamine chloride anesthesia, and all efforts were made to minimize suffering.

Animals and housing

The study population consisted of 143 male Wistar rats (Rattus norvegicus) aged 12-14 wk, weighing 300-350 g. Animals were kept in unisexual groups of four individuals from weaning (4wk after birth) until the onset of the experiments, in a temperature-controlled room at 22–24 ℃, with the light on between 7.00 AM and 7.00 PM. The bedding of the cages consisted of wood shavings, and food and water were freely available.

In 118 animals (Group D), diabetes was induced by a single intra-peritoneal injection of streptozotocin (STZ, 60 mg/kg) while the remaining 25 control rats (group C) were injected only with saline vehicle (0.9% NaCl). Glucose blood levels and body weights were measured in 2-hour-fasting animals, before STZ or vehicle injection, two days after injection, and then weekly until sacrifice.

D animals were either untreated (n=54) or subjected to chronic administration of (i) low doses of trans-Resveratrol (Sigma, Milan, Italy), (intraperitoneal injection: 2.5 mg/Kg/day; DR groups, n=64). The treatment started immediately after the documented increase in glucose blood levels (2 days after STZ injection).

Functional measurements and sacrifice were performed 1 week (D1, D1R groups), 3 weeks (D3, D3R) or 8 weeks (D8, D8R) after induction of hyperglycemia.

Functional measurements

Hemodynamic study

Invasive hemodynamic data were recorded in 83 rats (12 D1, 17 D1R, 10 D3, 13 D3R, 8 D8, 11 D8R, and 12 C). Each rat was anaesthetized with ketamine chloride 40 mg/kg i.p. (Imalgene, Merial, Milano, Italy), plus medetomidine hydrochloride 0.15 mg/kg ip (Domitor, Pfizer Italia S.r.l., Latina, Italy).

The right carotid artery was cannulated with a microtip pressure transducer catheter (Millar SPC-320, Millar Instruments, Houston, TX, USA) connected to a recording system (Power Laboratory ML 845/4 channels, 2Biological Instruments, Besozzo, Italy) and systolic and diastolic blood pressures were determined. The catheter was then advanced into the left ventricle to measure: 1) LV systolic pressure (LVSP), 2) LV end-diastolic pressure (LVEDP), 3) the peak rate of rise and decline of LV pressure (±dP/dt), taken as indexes of myocardial mechanical efficiency, 4) isovolumic contraction time (IVCT: duration of isovolumic contraction), and 5) LV relaxation time (LVRT), computed from –dP/dt to 5 mmHg above LVEDP [52] (software package CHART B4.2) (Fig. 5).

Then, the hearts of D, DR and C rats were divided in two subgroups and used for electrophoresis and immunoblot assay (n=3 for each group) or morphometric and immunohistochemical analyses (see below).

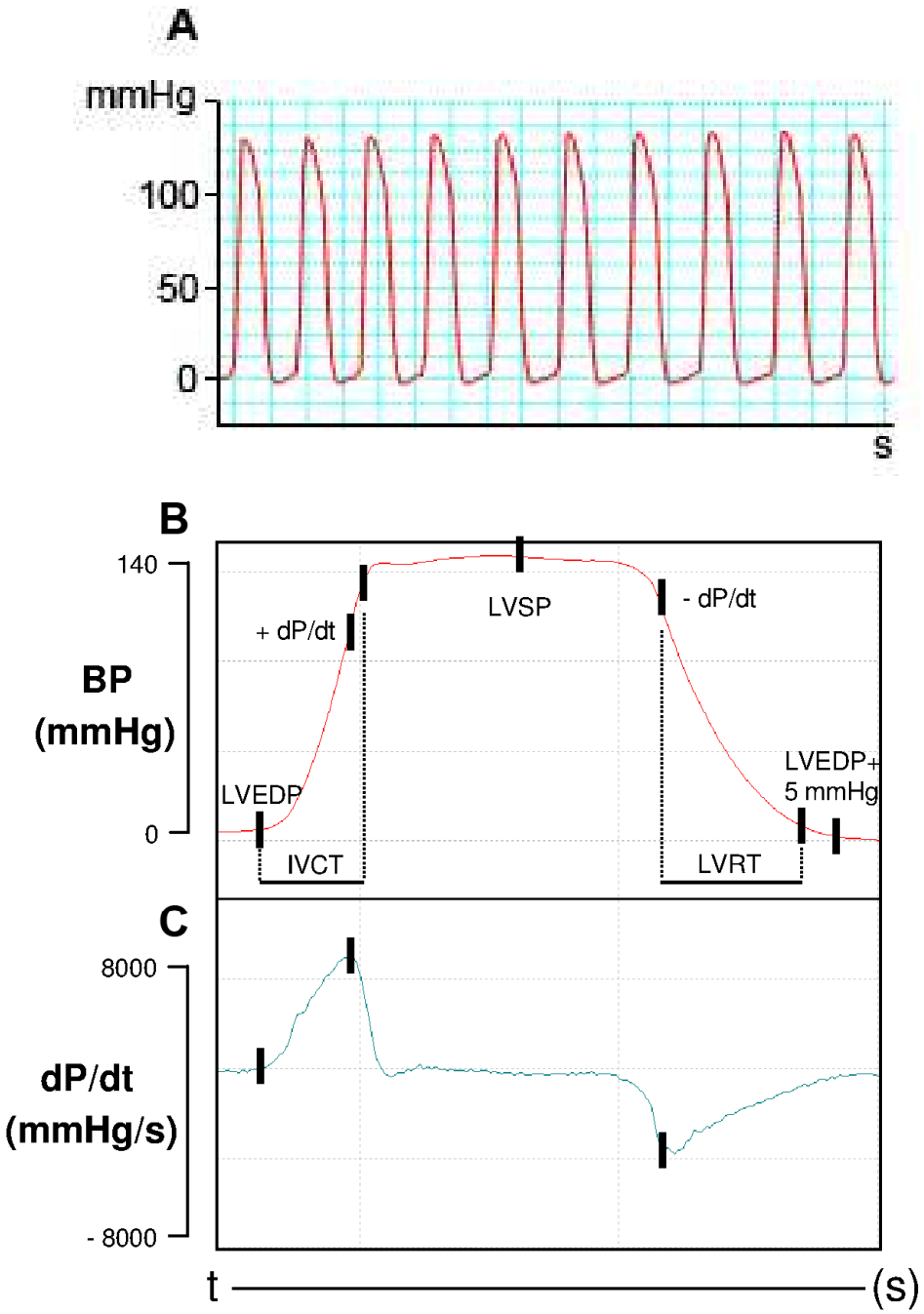

Figure 5. Tracing example of the left ventricular pressure recorded in one representative control rat in A. Enlargement of a single cardiac cycle in B and in C first derivative of the time function described in B.

Myocyte Isolation and measurement of cell mechanics

The remaining 60 rats were used for cardiomyocyte and CSPC isolation. From the hearts of 8 D1, 8 D1R, 8 D3, 9 D3R, 8 D8, 6 D8R, and 13 C rats, individual ventricular myocytes were enzymatically isolated by collagenase perfusion in accordance with a procedure previously described [53].

Briefly, the rat heart was removed and rapidly perfused at 37 ℃ by means of an aortic cannula with the following sequence of solutions: 1) a calcium-free solution for 5 min to remove the blood, 2) a low-calcium solution (0.1 mM) plus 1 mg/ml type 2 collagenase (Worthington Biochemical Corporation, Lakewood, NJ, USA), and 0.1 mg/ml type XIV protease (Sigma, Milan, Italy) for about 20 min; and 3) an enzyme-free, low-calcium solution for 5 min. Calcium-free solution contained the following (in mM): 126 NaCl, 22 dextrose, 5.0 $MgCl_2$, 4.4 KCl, 20 taurine, 5 creatine, 5 Na pyruvate, 1 NaH_2PO_4, and 24 HEPES (pH = 7.4, adjusted with NaOH), and the solution was gassed with 100% O_2.

The LV was then minced and shaken for 10 min. The cells were filtered through a nylon mesh and re-suspended in low-calcium solutions for 30 min. Then, cells were used for measuring sarcomere shortening and calcium transients.

Smears were also made, and LV cells were stained with toluidine-blue. For each group, 500 cells were analyzed by optical microscopy to calculate cell surface area (Fig. 6).

Mechanical properties of ventricular myocytes were assessed by using the IonOptix fluorescence and contractility systems (IonOptix, Milton, MA, USA).

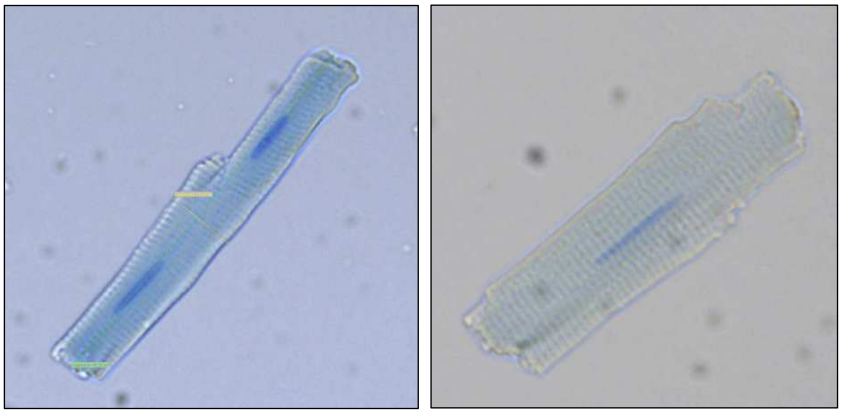

Figure 6. Smeared LV cardiomyocytes stained with toluidine-blue.

Sarcomere length. LV myocytes were placed in a chamber mounted on the stage of an inverted microscope (Nikon-Eclipse TE2000-U, Nikon Instruments, Florence, Italy) and superfused (1 ml/min at 37 ℃) with a Tyrode solution containing (in mM): 140 NaCl, 5.4 KCl, 1 $MgCl_2$, 5 HEPES, 5.5 glucose, and 1 $CaCl_2$ (pH 7.4, adjusted with NaOH).

Only rod-shaped myocytes with clear edges and average sarcomere length ≥ 1.7 µm were selected for the analysis. All the selected myocytes did not show spontaneous contractions. The cells were field stimulated at a frequency of 1 Hz by rectangular depolarizing pulses (2 ms in duration, and twice diastolic threshold in intensity) by platinum electrodes placed on opposite sides of the chamber, connected to a MyoPacer Field Stimulator (IonOptix). The stimulated myocyte was displayed on a computer monitor using an IonOptix MyoCam camera. Load-free contraction of myocytes was measured with the IonOptix system, which records the sarcomere pattern to calculate the changes in the sarcomere spacing with a fast Fourier transform algorithm. Then, frequency data were converted to length.

A total of 638 isolated ventricular myocytes were analyzed (125 from C hearts, 85 from D1, 80 from D3, 83 from D8, 111 from D1R, 95 from D3R and 59 from D8R) to assess cellular mechanical properties by computing the following parameters: mean diastolic sarcomere length, fraction of shortening (FS), and maximal rates of shortening and re-lengthening (±dL/dt).
Steady-state contraction of myocytes was achieved before data recording.

In 30 cells of each group, Ca^{2+} transients were measured simultaneously with mechanical properties. Ca^{2+} transients were determined by epifluorescence after loading the myocytes with 10 µM fluo 3-AM (Invitrogen, Carlsbad, CA) for 30 min. Excitation length was 480 nm, with emission collected at 535 nm using a X40 oil objective. Fluo 3 signals were expressed as normalized fluorescence (f/f0: fold increase). The time course of the fluorescence signal decay was described by a single exponential equation, and the time constant (Tau) was used as a measure of the rate of intracellular calcium clearing.

CSPC isolation and cell cultures

CSPC-isolation

CSPCs were enzimatically isolated from the heart of control rat hearts. The isolation procedure was the same as for cardiomyocytes, but ventricular fragments were maintained for a longer time in a collagenase+albumine solution at 37 °C to allow mechanical tissue dissoc iation. The solution containing all cells was washed several times, centrifuged at 300 rpm to remove cardiomyocytes, and then submitted to Percoll (Sigma, Milan, Italy) gradient to further enrich the fraction of small cells. The cell layer visualized at the interface of the desired gradient was centrifuged at 1000 rpm and cells re-suspended in 10 ml of culture medium containing Iscove Modified Dulbecco's Medium (IMDM, Sigma, Italy) supplemented with 1% Penicillin-Streptomycin (P/S, Sigma, Italy), 1% Insulin-Transferrin-Sodium Selenite (I/T/S, Sigma, Italy), 10% Fetal Bovine Serum (FBS, Sigma, Italy) and 10 ng/ml Basic-Fibroblast Growth Factor (b-FGF, Sigma, Italy) and seeded in Petri dishes (Corning, USA) placed at 37 °C-5% CO_2 for their amplification.

Daily, microscopic observation of cultures allowed the recognition of two different adherent cell populations, one with mesenchymal-like and one with monomorphic blast-like characteristics. This latter population constitutes the so-called Cardiac Progenitor Cells (CSPCs) which exhibits clonogenic growth and multipotency [54, 55]. These cells were amplified for several passages and cryo-preserved in aliquots in a medium composed by FBS supplemented with 1% Dimethylsulphoxide (DMSO, Sigma, Italy).

Co-cultures: CSPCs-cardiomyocytes

In order to evaluate whether and to which extent the functional properties of CSPCs were affected by parenchymal cells of RSV-treated and untreated hearts, control CSPCs (previously expanded from passage 1 to 4) were seeded at a concentration of 35,000/cm^2 together with ventricular cardiomyocytes (at a concentration of 18,000/cm^2) isolated from untreated and RSV-treated D1, D3 and D8 hearts (Fig. 7).

Growth (phospho-histone H3-positive CSPCs; polyclonal rabbit anti-ph-H3, Upstate, Charlottesville, VA, USA) and survival characteristics (TUNEL assay) of CSPCs were analyzed after 72 hours of co-culture.

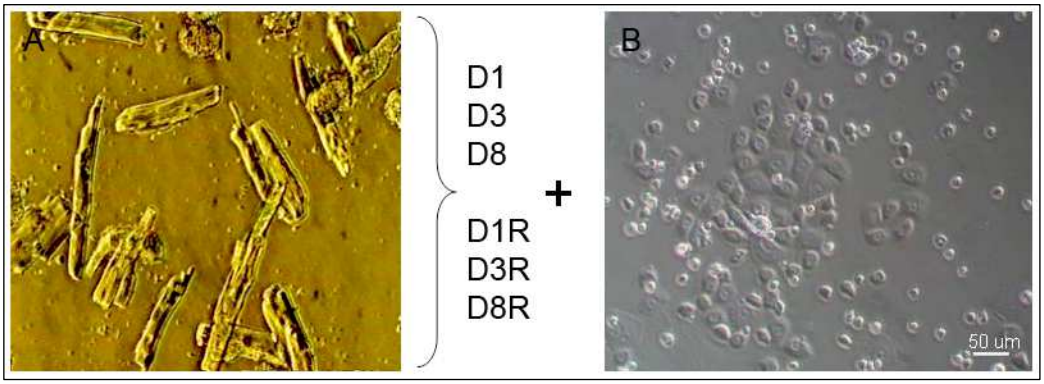

Figure 7. Examples of cultured isolated LV myocytes (A) and control CSPCs (B).

Analysis of conditioned media

The conditioned medium from each co-culture was harvested after 72 hours and evaluated using RayBio Rat Cytokine Antibody Array II purchased from RayBiotech (Norgross, GA, USA). This assay can simultaneously detect the expression level of different cytokines with high specificity. Briefly, after treating the membranes with a blocking buffer, 1 ml of conditioned medium was added and incubated at room temperature for 2 hours. The membranes were washed, and 1 ml of primary biotin-conjugated antibody was added and incubated at room temperature for 2 hours. Then, the membranes were incubated with 2 ml of horseradish peroxidase-conjugated streptavidin at room temperature for 1 hour and subsequently developed by using enhanced chemiluminescence-type solution (Immobilon Western-Millipore) and exposed to Kodack X-Omat AR film for an appropriate length of time (Fig. 8). The intensities of signals were quantified by densitometry (software for image capturing and analysis: ImageQuant- Molecular Dynamics). For each spot the net density was determined by subtracting the background gray levels. The density of the positive control spots were used to normalize the results from the different membranes.

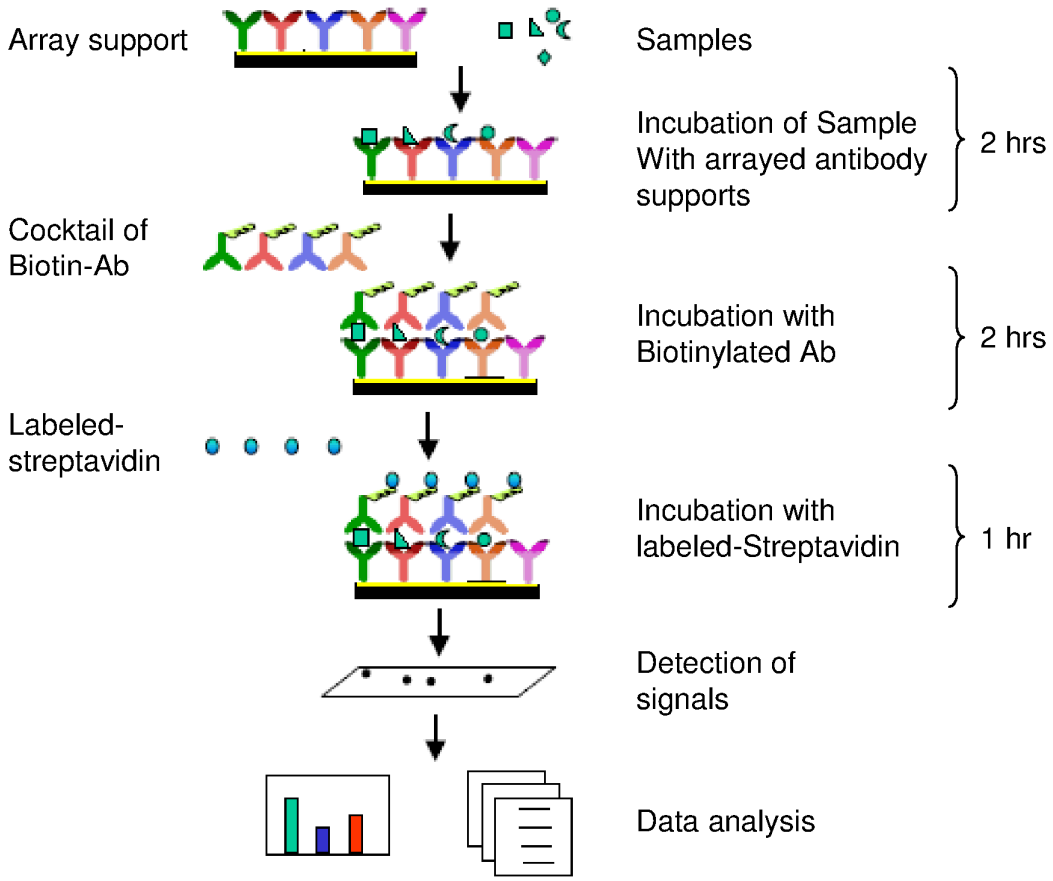

Figure 8. Rat Cytokine antibody array II working procedure.

Cardiac anatomy and morphometry

In 9 C, 9 D1, 14 D1R, 7 D3, 10 D3R, 5 D8 and 8 D8R rats, the abdominal aorta was cannulated, the heart was arrested in diastole with injection of $CdCl_2$ solution (100 mM), and the myocardium was retrogradely perfused with 10% buffered formalin solution. The left ventricular chamber was filled with fixative at a pressure equal to the in vivo measured systolic pressure. The heart was then excised and placed in formalin solution (10%) for 24 hours.

Cardiac anatomy. The right ventricle (RV) and the left ventricle (LV) inclusive of the septum were separately weighed and the volume of the left ventricular myocardium was computed by dividing LV myocardial weight by the specific weight of the tissue (1.06 g/ml). LV chamber length was measured from the apex to the aortic valve. A 1-mm-thick transverse slice was cut from the mid-region of the LV and used to compute LV wall thickness and chamber equatorial diameter (Image Pro-plus, Media Cybernetics, Bethesda, MD, USA, version 7.0). The LV chamber volume was calculated according to the Dodge equation which equalizes the ventricular cavity to an ellipsoid [56]. The slice was then embedded in paraffin and five-micrometer-thick sections were cut and used for morphometric and immunohistochemical analyses.

Morphometric analysis. Sections were stained with Masson's trichrome and analyzed by optical microscopy (magnification 250X) in order to evaluate in the ventricular myocardium: (i) the volume fraction of myocytes, (ii) the volume fraction of interstitial and perivascular fibrosis, and (iii) the numerical density and average cross-sectional area of fibrotic foci. According to a procedure previously described [57], for each section, these analyses were performed in 60 adjacent fields from sub-endocardium, mid-myocardium and sub-epicardium. The measurements were obtained with the aid of a grid defining a tissue area of 0.160 mm^2 and containing 42 sampling points each covering an area of 0.0038 mm^2.

Immunohistochemistry

Atrial and LV sections were analyzed to estimate (i) the percentage of apoptotic cells (TUNEL assay), (ii) the numerical density of cells expressing c-kit, the receptor for Stem Cell Factor (rabbit polyclonal anti-c-kit antibody, Santacruz Biotecnology, Santa Cruz, CA, USA), (iii) the arteriolar and capillary density (mouse monoclonal anti-alpha-smooth muscle actin antibody and rabbit polyclonal anti-vW factor, Dako, Glostrup, Denmark); (iv) the relative expression of alpha cardiac isoforms [58] by using specific antibodies against α-smooth muscle actin (α-SMA), α-cardiac actin (α-CA) and α-skeletal actin (α-SKA). All these antibodies have been developed and characterized in the Dept. of Pathology and Immunology, University of Geneva, Switzerland [59, 60, 61]

Electrophoresis and immunoblot assay

In 3 rats for each group, the hearts were excised, and the left and right ventricles were weighed and immediately frozen at -80 ℃. Western blot assay was used to assess the expression levels of high-mobility group box-1 protein (HMGB-1) as an index of activation of pro-inflammatory signal cascades in ventricular myocardial tissue.

The left ventricular tissue was mechanically fragmented in liquid nitrogen, homogenized in Sample Buffer (62.5 mM Tris-HCl, pH 6.8, 2% sodium dodecyl sulfate (SDS), 10% glycerol, 50 mM DTT, 0.01% bromophenol blue) and boiled for 5 min. For each animal, 50 µg of proteins were separated on 10% polyacrylamide gels and electroblotted on nitrocellulose membranes (Protran, Schleicher & Schuell, Dassel, Germany). Membranes were blocked with 5% milk in TBS-T (Tris-Buffered Saline Tween-20) and were incubated overnight at 4 ℃ with the primary antibody (anti-HMGB1 rabbit p olyclonal antibody, Abcam, Cambridge, UK). After washing the membranes, a second incubation was performed for one hour at room temperature with peroxidase conjugated affinity purified goat anti-rabbit secondary antibody (Jackson Immunoresearch Laboratories, West Grove, PA). Peroxidase activity was developed using the ECL Western blotting system (Amersham, Rahn AG, Zürich, Switzerland), according to the instructions of the manufacturer. To determine the expression levels of HMGB-1, blots were scanned and the intensity of the band was

quantified by means of the ImageJ Program (NIH, Bethesda, MD, USA). Actin (anti-actin rabbit polyclonal antibody, Sigma) was used as the loading control.

Statistical analysis

Power analysis has been performed to evaluate the research design and minimize Type II errors and sample size. Preliminary hemodynamic data obtained in a pilot study have been used. The ANOVA statistical test was used for computing the F value, the significance level, the effect size and the non-centrality parameter (PASW Statistics 18). Then, a-priori power analysis was used (G*Power Version 3.1.2; Franz Faul, Kiel University, Germany) by setting $\alpha=0.01$ and $\beta=0.05$ (power $1-\beta=0.95$) in accordance with the suggestion of Cohen [62], to estimate total sample size and the number of measurements required for each group. Statistics of variables included mean±standard error (SE), Multifactorial analysis of variance (1 way ANOVA followed by Bonferroni's post-hoc test or Dunnett's test when appropriate). Statistical significance was set at $p<0.05$.

Glucose blood levels and body weight

At the beginning of the experimental protocol, glucose blood levels and body weight ranged respectively between 102-109 mg/dl and 301-445 g, in the entire rat population. In D animals, after STZ injection, glucose blood levels were higher than those measured in C group, at every time points of observation (Table 1). In addition, body weight decreased by 15% during the first week of hyperglycemia to remain essentially constant until 8 weeks (Table 1). RSV treatment did not significantly affect both glucose blood levels and body weight (Table 1).

Body weight and glucose blood levels

	BW (g)	Glucose blood levels (mg/dl)
1 week		
C	403±13	92±1
D1	348±6 *	494±18 *
D1R	341±5 *	473±17 *
3 weeks		
C	410±14	105±1.5
D3	337±7 *	491±23 *
D3R	327±5 *	517±14 *
8 weeks		
C	419±10	103±3
D8	331±8 *	525±20 *
D8R	321±5 *	545±21 *

Table 1. Values are mean ± SE of body weight (BW) and glucose blood levels measured in control (C), diabetic (D) and RSV-treated diabetic rats (DR), at 1-3-8 weeks after STZ or vehicle injection. * $p < 0.01$ significant differences vs. C animals.

Hemodynamics

Heart rate measured under anesthesia was similar in all experimental groups (heart rate ranging from 195 and 220 beats/minute, in the different groups). In comparison with C rats, all diabetic groups exhibited significantly lower values of systolic LV pressure (range: 103-112 mmHg vs. 133 mmHg measured in C) (Fig. 9) while end-diastolic pressure was unchanged (range: 5-9 mmHg). Marked signs of systolic and diastolic ventricular dysfunction developed after 8 weeks of diabetes, including a significant reduction in ±dP/dt (Fig. 10 A-B), associated with a prolongation of both isovolumic contraction time (IVCT) and relaxation time (LVRT) (Fig. 10 C-D).

In D8R group, RSV treatment abolished the negative impact of diabetes on LV hemodynamics and all parameters reached control values with the exception of the rate of pressure decline during relaxation (-dP/dt) (Fig. 10 B).

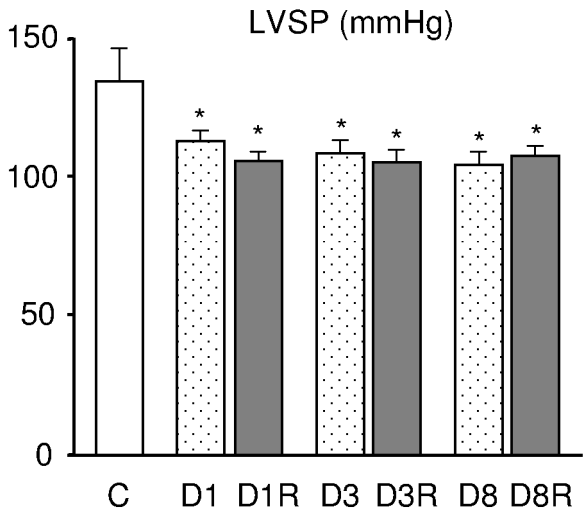

Figure 9. Hemodynamic measurements

Mean values ± SE of left ventricular systolic pressure (LVSP). * $p < 0.01$: significant differences vs. C.

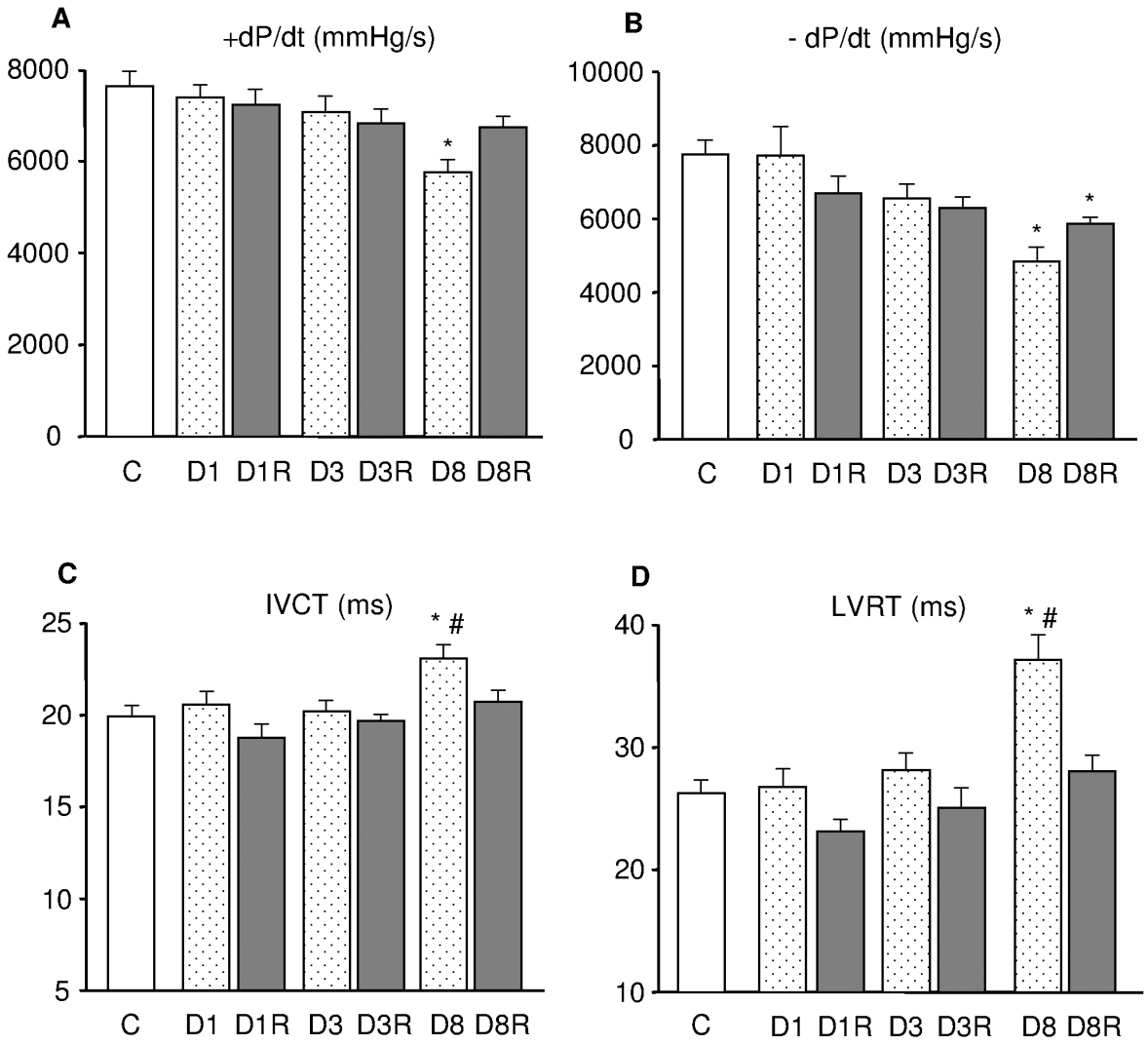

Figure 10. Hemodynamic measurements

Mean values ± SE of: A) maximum rate of ventricular pressure rise (+dP/dt), B) maximum rate of ventricular pressure reduction (-dP/dt), C) isovolumic contraction time (IVCT), and D) LV relaxation time (LVRT), measured in control rats (C) and untreated or RSV-treated diabetic rats after 1 (D1, D1R), 3 (D3, D3R) and 8 (D8, D8R) weeks of hyperglycemia. * $p < 0.01$: significant differences vs. C; # $p < 0.05$: significant differences between D8 and D8R.

Cell mechanics and calcium transients

Globally, 638 isolated ventricular myocytes were used for cell mechanics (125 from C hearts, 85 from D1, 80 from D3, 83 from D8, 111 from D1R, 95 from D3R and 59 from D8R). In 30 cells of each experimental group, calcium transients were simultaneously recorded. The average diastolic sarcomere length was comparable in all groups (average sarcomere length equal to 1.71±0.001 µm).

In accordance with the *in vivo* recorded hemodynamic data, the mechanical properties of ventricular myocytes from D1 and D3 diabetic hearts were globally preserved (Fig. 11 B-D), except for the lower rate of intracellular calcium clearing (Tau) in D3 (Fig. 12 B). Conversely, a definite worsening of cell mechanics occurred in D8 (Fig. 11 A-D). In comparison with C cells, D8 cardiomyocytes exhibited a reduced fraction of shortening associated with a significant decrease in the maximal rate of shortening (-dL/dt) and relengthening (+dL/dt) ($p<0.01$; Fig. 11 B-D). The impaired contractility in D8 cells was accompanied by a significant decrease in calcium transient amplitude (f/f0) (-15%, $p<0.01$; Fig. 12 A) and a prolonged Tau (+50%, $p<0.01$; Fig. 12 B). The progressive impairment of cardiomyocyte contractile efficiency produced by diabetes was partially improved by RSV treatment as shown by the recovery of fraction of shortening (Fig. 11 B) and f/f0 (Fig. 12 A).

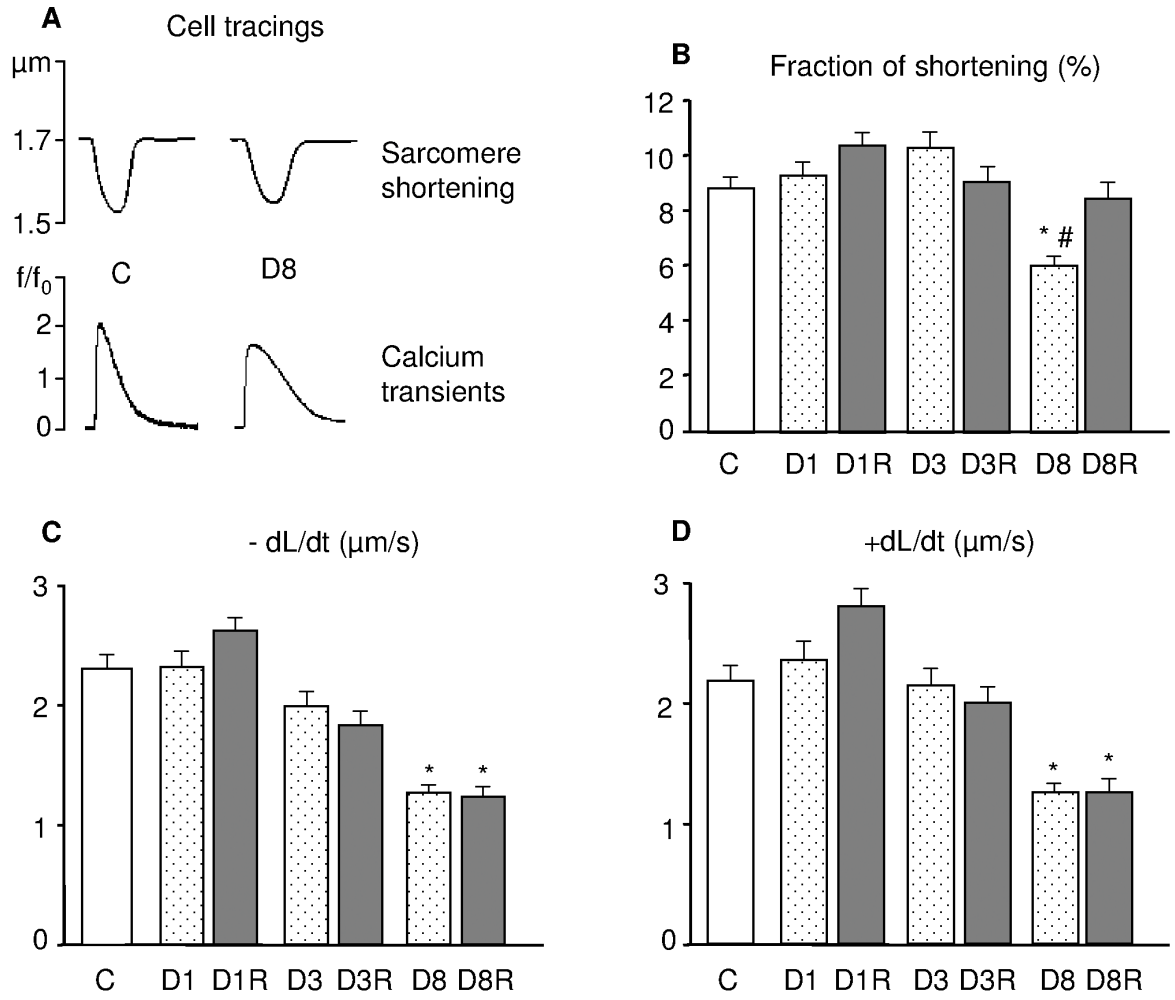

Figure 11. Cell mechanics

A) Representative examples of sarcomere shortening and corresponding calcium transients (normalized tracings: fold increase) recorded from C and D8 ventricular myocytes. In bar graphs, the mean values ± SE of: B) sarcomere fraction of shortening, C) maximal rate of shortening (-dL/dt), D) maximal rate of relengthening (+dL/dt), measured in control myocytes (C), and untreated or RSV-treated diabetic cells (D and DR, respectively), after 1, 3 and 8 weeks of hyperglycemia.

* $p < 0.01$: significant differences vs. C; # $p < 0.05$: significant differences between D8 and D8R.

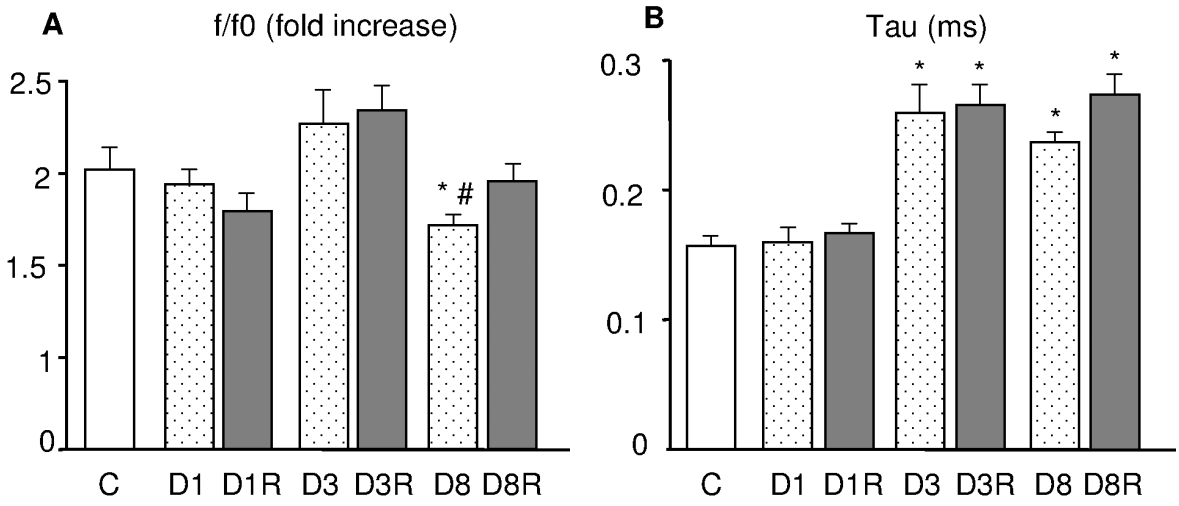

***Figure 12*.** Intracellular calcium transients

In bar graphs, the mean values ± SE of: A) calcium transient amplitude expressed as peak fluorescence normalized to baseline fluorescence (f/f0) and B) time constant of the intracellular calcium decay (Tau), measured in control myocytes (C), and untreated or RSV-treated diabetic cells (D and DR, respectively), after 1, 3 and 8 weeks of hyperglycemia.

* $p < 0.01$: significant differences vs. C; # $p < 0.05$: significant differences between D8 and D8R.

Effects of diabetes and RSV on cardiac anatomy and myocardial tissue

Diabetes induced a marked loss of left ventricular mass in D1, D3 and D8 untreated hearts ($p<0.05$; Fig. 13 A), in the absence of significant changes in individual cardiomyocyte size (average cardiomyocyte surface area: approximately 1,400 μm^2, data not shown). A significant dilation of LV chamber was observed only after 8 weeks of diabetes (Fig. 13 B) leading to a marked reduction in mass-to-chamber volume ratio in D8 group (Fig. 13 C). These unfavorable anatomical changes produced by diabetes were reversed by RSV administration (Fig. 13 A-C).

The total amount of collagen accumulation was negligible and similar to control ventricles in RSV-treated and untreated diabetic hearts during the first 3 weeks of hyperglycemia. In D8 group, although myocardial damage was still limited, the total amount of fibrosis in the myocardium was significantly increased in comparison with C (Fig. 14 A). Perivascular fibrosis was observed in association with small foci of reparative fibrosis characterized by inflammatory cellular infiltrates (Fig. 14 B-C), more evident in the mid-myocardium. The activation of pro-inflammatory signal cascades was confirmed by the significant increase in HMGB-1 expression in D8 group, as revealed by Western blotting assay (Fig. 15). Cardiac damage and inflammation signals were completely prevented by RSV administration (Fig. 14 A, 15).

Significantly lower values of α-SKA expression were also detected in diabetic cardiomyocytes, after 3 and 8 weeks of hyperglycemia (-50% on average in both groups vs. C; Fig. 16 A-B). This reduction was counteracted by RSV-treatment in D3R group (Fig. 16 A-B) while the effect of RSV was less evident at the later time point (D8R group).

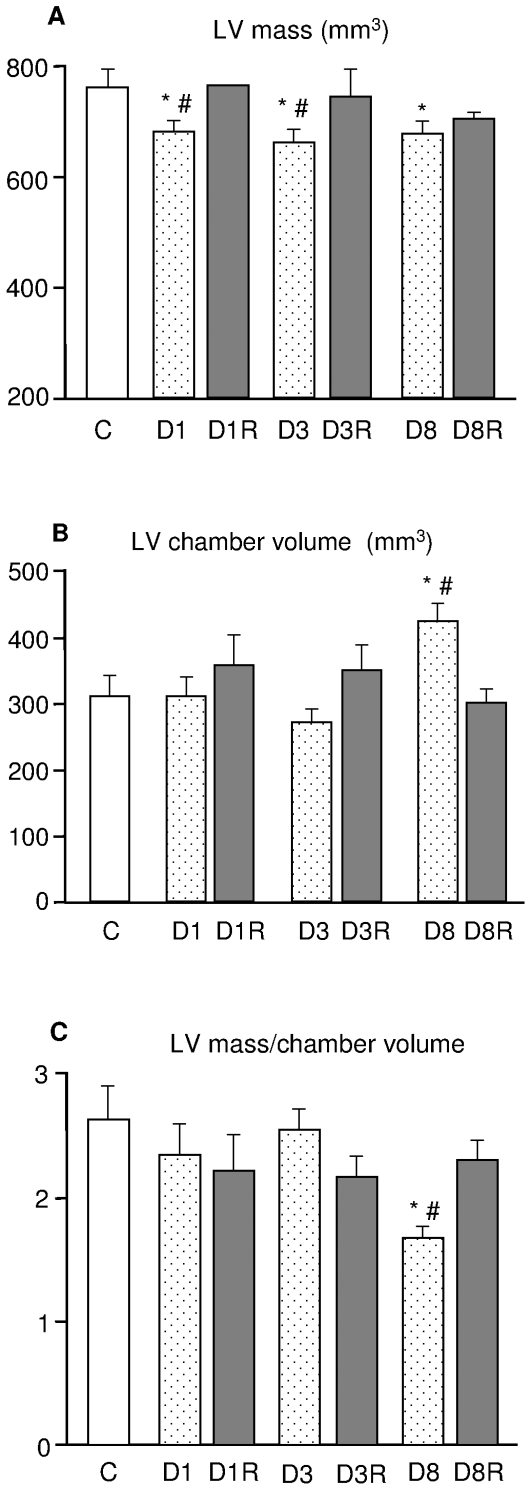

Figure 13. Cardiac anatomy and tissue morphometry

In A-C graphs the mean values ± SE of the left ventricular (LV) geometrical properties measured in the different experimental groups: A) LV mass, B) LV chamber volume, and C) LV mass to chamber volume ratio.

* $p < 0.05$: significant differences vs. C; # $p < 0.05$: significant differences vs. the corresponding RSV-treated group.

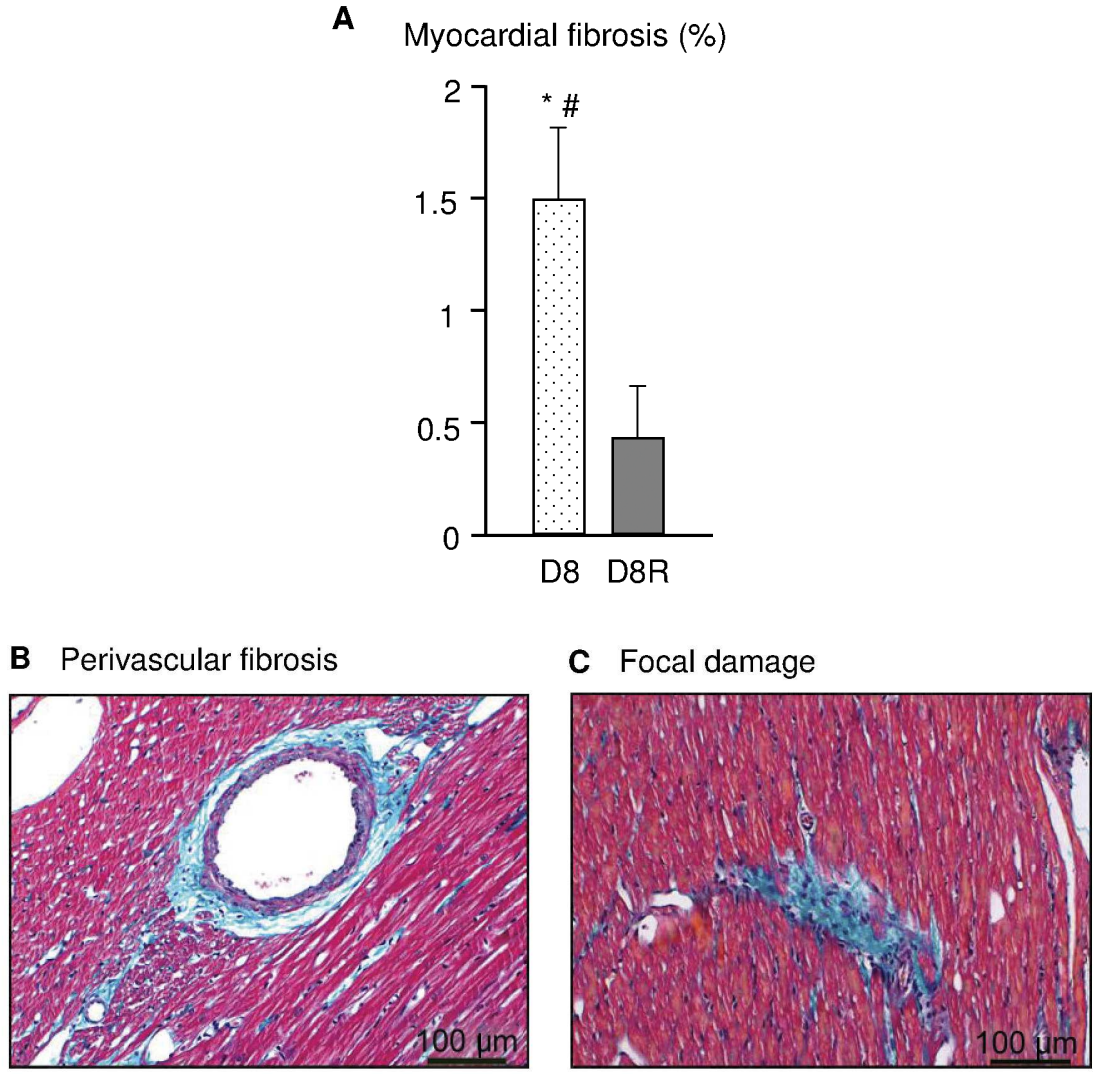

Figure 14. Cardiac anatomy and tissue morphometry

In A) mean values ± SE of the volume fraction of fibrosis morphometrically determined in D8 and D8R groups. B-C: sections of LV mid-myocardium stained with Masson's trichrome showing in greenish blue the fibrotic tissue in a D8 rat heart. B: accumulation of collagen in perivascular space. C: focal damage characterized by the presence of collagen and inflammatory cell infiltrate. Scale bars = 100 µm.

* $p < 0.05$: significant differences vs. C; # $p < 0.05$: significant differences vs. the corresponding RSV-treated group.

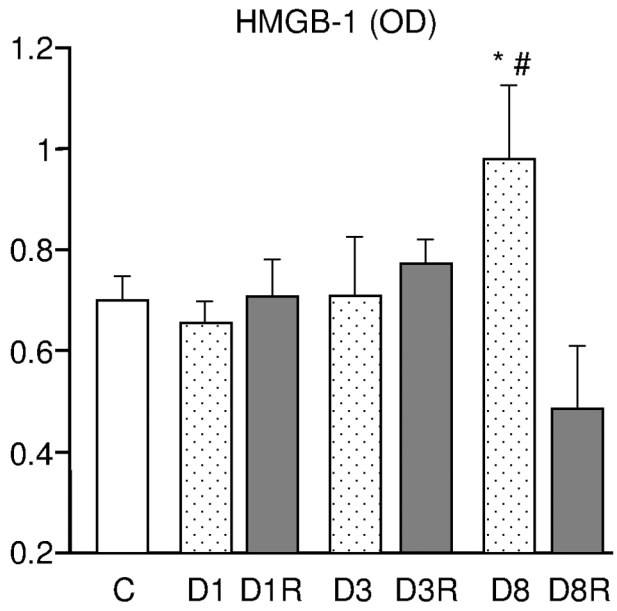

Figure 15. HMGB-1 expression in left ventricular myocardium

Expression levels of high mobility group box-1 protein (HMGB-1) in left ventricular myocardium. OD: optical density. Data are reported as mean ± SE.

* $p < 0.01$: significant differences vs. C; # $p < 0.05$: significant differences vs. the corresponding RSV-treated group.

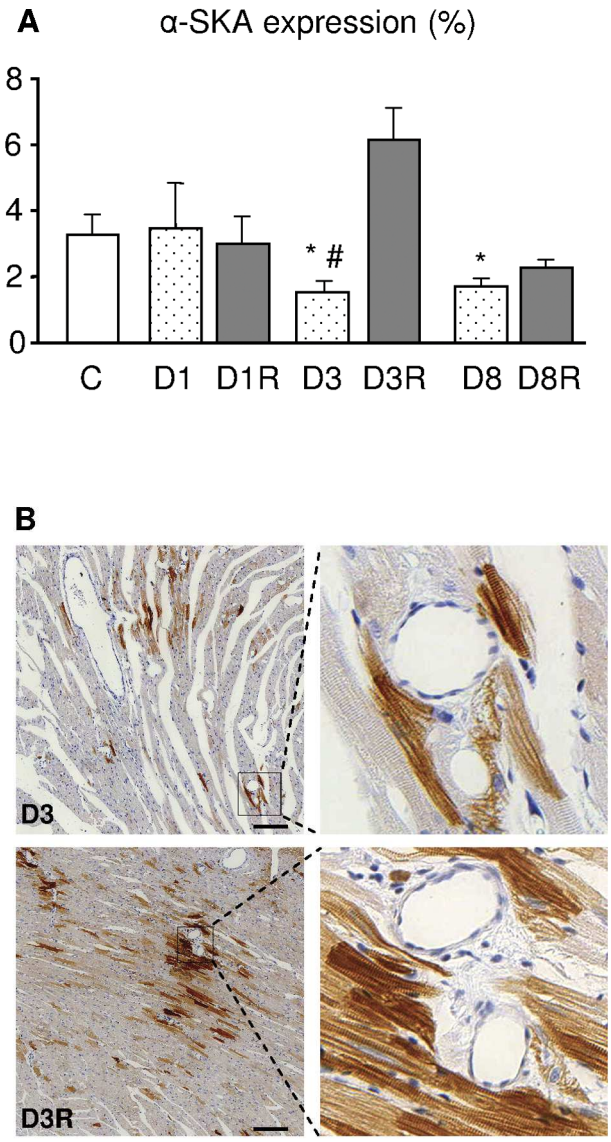

Figure 16. Alpha-SKA expression in left ventricular myocardium

A) Expression levels of α-SKA in left ventricular myocardial tissue. Data are reported as mean ± SE. * $p < 0.01$: significant differences vs. C; # $p < 0.05$: significant differences vs. the corresponding RSV-treated group.

B) Sections of D3 (upper panels) and D3R (lower panels) LV myocardium stained with anti α-SKA. Black squares inscribe an area shown at higher magnification in the corresponding adjacent panels. Scale bar = 100 μm.

Effects of RSV on diabetes-induced cardiomyocyte and endothelial cell apoptosis

To determine ongoing apoptotic cell death, tissue sections of the LV myocardium were subjected to the TUNEL assay. In comparison with control hearts, the percentage of apoptotic cardiomyocytes increased with diabetes at all time points of observation (Fig. 17 A) while apoptosis in endothelial cells increased from 3 to 8 weeks (Fig. 17 B). Overall, RSV treatment was able to reduce by 65% to 85% the incidence of apoptotic cell death (Fig. 17 A-B) although, after 8 weeks of diabetes, a marked protective effect was maintained only on endothelial cells (Fig. 17 B).

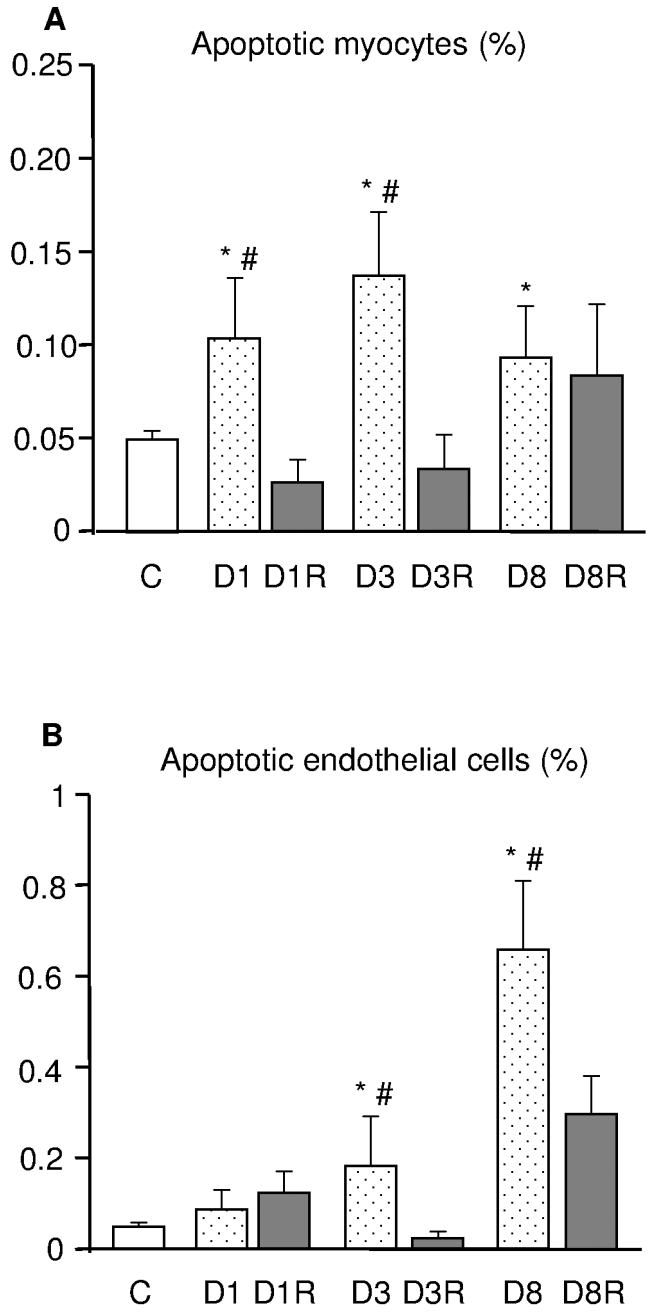

Figure 17. Effects of diabetes and RSV on myocardial cell apoptosis

Bar graphs illustrate the percentage of apoptotic cardiomyocytes (A) and endothelial cells (B). Data are expressed as mean values ± SE.

* $p < 0.01$: significant differences vs. C; # $p < 0.05$: significant differences vs. the corresponding RSV-treated group.

Effects of diabetes and RSV treatment on CSPCs

Tissue analysis

To evaluate the effects of diabetes and RSV treatment on the numerical density and tissue distribution of CSPCs, sections of the atria and LV from all experimental groups were immunostained for the detection of c-kit, the receptor of Stem Cell Factor, representing the most preserved stem cell antigen among different tissues of different species [63].

As expected, the quantitative analysis documented that in control hearts the number of c-kit-positive CSPCs was 2.5 fold higher in the atria with respect to the LV supporting the notion of preferential sites of accumulation of cardiac primitive cells [28]. Diabetes significantly reduced the density of CSPCs in the atrial appendages at all time points (Fig. 18 A). Conversely, the deleterious effect of diabetes on left ventricular CSPCs was detected only after 8 weeks of hyperglycemia (Fig. 18 B). RSV administration significantly attenuated the early and late dramatic depletion of CSPCs from the atrial sites of storage (Fig. 18 A), although was not able to counteract the late diabetes-induced loss of progenitor cell compartments in the working left ventricle (Fig. 18 B).

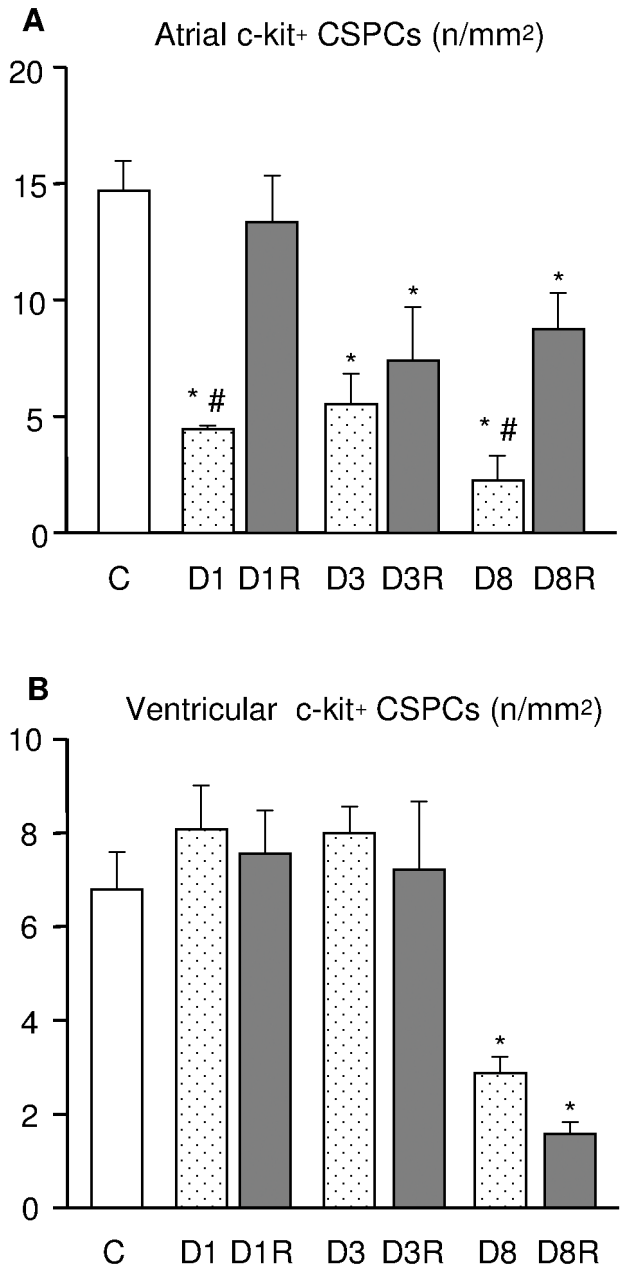

Figure 18. Effects of diabetes and RSV on CSPC number

Bar graphs illustrate the numerical density of atrial (A) and ventricular (A) c-kit+ CSPCs. OD: optical density. Data are expressed as mean values ± SE.

* $p < 0.01$: significant differences vs. C; # $p < 0.05$: significant differences vs. the corresponding RSV-treated group.

In vitro analysis

It is well established that, especially at the level of niches, stem cell function is tightly regulated by environmental factors [29]. Thus, we determined *in vitro* whether the negative impact of diabetes and the protective action of RSV on CSPCs could be attributed to changes in myocardial environment. Specifically, the effect of diabetic cardiomyocytes, isolated from RSV-treated and untreated diabetic hearts, on the magnitude of CSPCs apoptotic death (TUNEL) and proliferation (Ph-H3) was analyzed.

CSPCs co-cultured with D1, D3 or D8 diabetic cardiomyocytes exhibited a higher rate of death associated with a lower proliferation capacity leading to an increased death-to-proliferation ratio, in comparison with CSPCs co-cultured with RSV-treated cardiomyocytes, at all time points of observation (Fig. 19 A). However, no linear relationship with the duration of diabetes was observed on this parameter. These *in vitro* observations suggest that the diabetic “milieu” impairs CSPC turnover which can be reversed by RSV. To investigate this phenomenon, we determined the relative concentrations of several cytokines in the media harvested from each co-culture condition.

The presence of cardiomyocytes isolated from D1 and D3 untreated diabetic hearts mainly resulted in a higher concentration of the monocyte chemotactic protein-1 (MCP-1) as compared with the conditioned media collected from co-cultures containing RSV-treated cardiomyocytes (D1R, D3R; Fig. 19 B). These data suggest that the inflammatory and pro-apoptotic bulk produced by diabetes can be attenuated by chronic RSV administration.

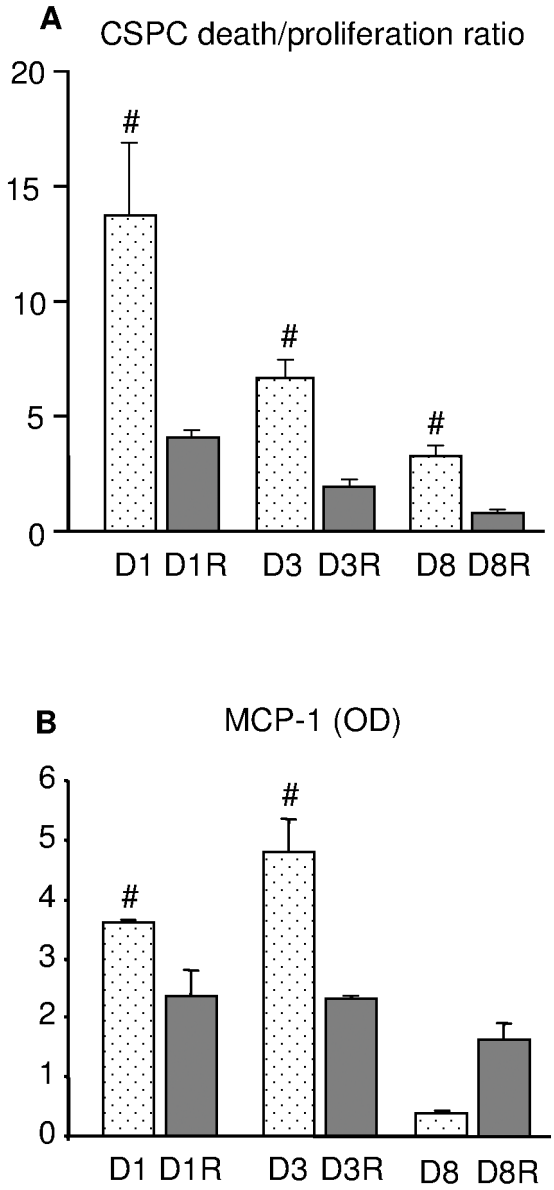

Figure 19. Co-cultures of CSPCs and cardiomyocytes

A: death to proliferation ratio of CSPCs co-cultured with untreated or RSV treated diabetic cardiomyocytes; B: concentration of the pro-inflammatory cytokine monocyte chemotactic protein-1 (MCP-1) in media harvested from co-cultures at different experimental time points. OD: optical density. Data are expressed as mean values ± SE. # $p < 0.05$: significant differences vs. co-cultures containing RSV-treated myocytes.

General Discussion and Conclusions

Diabetic cardiomyopathy refers to a distinct primary disease process which develops secondary to a metabolic insult and affects the myocardium causing a wide range of structural alterations and diastolic and systolic dysfunction or a combination of these, ultimately leading to heart failure. The appearance of diabetes is the factor which induces changes at the cellular level including chronic loss of myocytes and vascular cells with a decrease in muscle mass, chamber dilation and altered extracellular matrix, with consequential structural and functional abnormalities.

Accumulating evidence supports the concept that a “cardiac stem cell compartment disease” plays an important role in the pathophysiology of diabetic cardiomyopathy [30]. In the diabetic heart, enhanced oxidative stress and inflammation induces an imbalance between cell death and cell regeneration.

The death of mature myocytes, smooth muscle cells, and endothelial cells is the initiating factor but the progression of the diabetic cardiomyopathy is mediated by premature cellular aging and CSPCs’ death. The loss of CSPCs favors cellular senescence and may promote a shift in the pattern of cell death from apoptosis to necrosis within the myocardium. Accumulation of old cells and cell necrosis alter the orderly organization of myocardial structure, depressing cardiac performance. Cellular senescence and attrition of the pool of functionally competent CSPCs lead to an insufficient replacement of old, dying cells and the acquisition of the heart senescent phenotype. Therefore, in the diabetic cardiomyopathy the cardiac stem/progenitor cell compartments participate in the pathophysiology of DCM favoring its onset and its progression towards heart failure [64]. Thus, the preservation of CSPC compartment can contribute to counteract the negative impact of diabetes on the myocardium.

In the present study, we show that early treatment of diabetic rats with the natural polyphenolic compound Resveratrol, in addition to the protective effect on mature myocardial tissue, improves “myocardial diabetic milieu” and positively interferes with CSPC survival and functional properties, resulting in a decreased ventricular remodeling as compared with untreated animals. The functional counterpart of these effects is the recovery of cardiac hemodynamics associated with an improvement of cardiomyocyte mechanical properties.

Despite several experimental studies suggesting that antioxidants reduce diabetic cardiovascular complications, results from clinical trials have been

disappointing [65, 66] probably because traditional antioxidants have a scavenging action on already formed ROS but limited effects on their intracellular production [65].

Here, we tested the hypothesis that early administration of RSV can be efficient in preventing diabetic cardiomyopathy. In comparison with conventional antioxidant compounds, RSV holds great promise in the treatment of cardiovascular complications of diabetes due to its well known effects on several target molecules resulting in reduced inflammation and intracellular ROS production, inhibiting both mitochondrial ROS production and permeability transition thus protecting the key intracellular organelle against the oxidative stress [67]. RSV was also shown to (i) decrease the rate of apoptotic cell death, (ii) increase cellular expression of survival proteins, and (iii) enhance stem cell survival and cardiac regeneration in ischemic heart [41, 68-72].

RSV, as other natural polyphenolic compounds, at low doses promotes antioxidant effects and induces survival signals resulting in cardioprotection.

The protective role of RSV treatment was documented by the improved post-ischemic ventricular function and reduced myocardial infarct size and apoptotic cardiomyocytes and further supported by the generation of survival signals as evidenced by increased phosphorylation of Akt and activation of Bcl-2 [73]. On the contrary, at higher doses (>5 mg/kg/die), RSV has detrimental cellular effects with a pro-oxidant role followed by cell damage, p-Akt down-regulation and apoptosis [74]. Thus, we performed preliminary experiments in normal and diabetic animals in order to determine the best dose able to produce cardioprotection without eliciting toxic effects. The best suitable dose was fixed at 2.5 mg/Kg/day, delivered by intra-peritoneal injection, in accordance with data previously reported [73].

Under physiological conditions, reactive oxygen species (ROS), such as superoxide radical, hydroxyl radical, and hydrogen peroxide (H_2O_2) are continuosly produced in many cells, but ROS levels are regulated by a number of enzymes and physiological antioxidants, such as superoxide dismutase, glutathione peroxidase, catalase, and thioredoxin. However when the production of ROS becomes excessive, oxidative stress will develop and impose a harmful effect on the functional integrity of biological tissues. The generation of ROS is increased in both types of diabetes leading to cell dysfunction and apoptosis [50, 64, 75]. Moreover it has been postulated that

hyperglycemia, a key clinical manifestation of diabetes, affects several other mechanisms leading to the generation of advanced glycation end-products (AGEs) and activation of diacylglycerol (DAG)-protein kinase C (PKC), resulting in chronic inflammation [65, 76]. This unfavorable tissue environment, besides inducing myocyte/endothelial cell damage, can impair mobilization, survival and proliferation of CSPCs. In accordance with previous reports [29, 30], we found a progressive reduction in CSPC density both in atrial storage and ventricular myocardial tissue of diabetic rats, partially reverted by RSV administration. The critical role played by the adverse tissue environment on CSPC survival and proliferation was also supported by data obtained in the co-cultures of healthy CSPCs and cardiomyocytes isolated from diabetic rats.

Co-culture conditioned media showed a high concentration of the pro-inflammatory cytokine monocyte chemotactic protein-1 (MCP-1). It has been recently shown [77] that hyperglicemia induces the expression of MCP-1 and MCP-1 induces a novel zinc-finger protein termed MCP-1-induced protein (MCPIP) leading to oxidative stress via iNOS or NADPH oxidase. Oxidative stress results in increased endoplasmic reticulum stress, autophagy and cardiomyocyte death, thus playing a critical role in the pathophysiological progression of diabetic cardiomyopathy [77].

Systemic RSV treatment resulted in a reduced activation of pro-inflammatory pathways, as indicated by the lower levels of MCP-1 in the co-culture supernatant. A reduced tissue inflammation was also confirmed by the decreased inflammatory cell infiltration and lower expression of HMGB-1 in the ventricular myocardium, after 8 weeks of diabetes. HMGB-1, besides its well known nuclear function in transcription regulation, modifying the structure of DNA and stabilizing nucleosomes [78, 79], possesses an extracellular role as pro-inflammatory cytokine [80].

HMGB-1 can be secreted from cells in two ways, either passively or actively and can play a role as an initiator of inflammation through its passive release from necrotic cells or as a late promoter through its active secretion by activated immune cells such as macrophages and monocytes [81, 82]. The decrease in HMGB-1 expression in D8R is supposedly due to the reduction of both cardiac cell death and recruitment of inflammatory cells following RSV administration. Oxidative stress and tissue inflammation represent important factors leading to lesions of small coronary arteries and appearance of

perivascular/interstitial fibrosis occurring in diabetic patients and in experimental models of diabetes [64]. The antioxidant effect of RSV associated with the decrease in the pro-inflammatory “milieu” may account for the preservation of ventricular mass and the decreased fibrotic damage observed in treated hearts, resulting in attenuation of cardiac remodeling and improved myocardial function.

Our results also indicate that diabetes affects the expression of α-SKA in ventricular cardiomyocytes. During adult life, α-CA is the major actin isoform present and is uniformly expressed in myofibrils. On the contrary the expression of α-SKA is low and the distribution appears focal and represents about 5% of the total actin [51]. Previous studies showed that a higher α-SKA content is associated with faster heart dynamics [83] and may constitute a compensation mechanism to maintain cross-bridge turnover rate and achieve a high degree of myocardial contractility in pressure-overload cardiac hypertrophy [57]. Here, we found a significant reduction in α-SKA levels after 3 and 8 weeks of hyperglycemia while RSV treatment produced a recovery of α-SKA expression. Although this effect was much more evident after 3 weeks of diabetes and decreased with time, the early increment in α-SKA levels might contribute to maintain a proper answer to increased workload with a concurrent recovery of hemodynamic performance and cardiomyocyte mechanical properties during contraction, as observed at 8 weeks of diabetes.

Our results support the assumption that RSV treatment preserves the numerical density and functional abilities of both mature cardiac cells and atrial CSPC storage, improves cardiac microenvironment and reduces unfavorable ventricular remodeling, thus leading to a marked recovery of ventricular function which was almost complete at the organ level (hemodynamics) but only partial at the cellular level. It is conceivable that combining RSV administration with traditional therapies, reducing metabolic derangements and glucose blood levels, and strategies aimed at enhancing RSV bioavailability [84, 85] can increase and prolong the positive effects of the compound. In conclusion, our findings indicate that RSV administration can constitute an adjuvant therapeutic option in the prevention and treatment of DCM opening new perspectives for pharmaceutical interventions in degenerative heart diseases, based on natural polyphenolic compounds.

Future perspectives

Large number of scientific studies have reported that Resveratrol has a broad range of desiderable biological actions with beneficial potentials for human health, which include anti-oxidant, anti-inflammatory, cardio-protective and anti-tumor activities, supporting the idea that this dietary chemical may be a useful protective agent.

In the present work we demonstrated that RSV holds great promise in the prevention and treatment of DCM by regulating several target molecules that preserve the myocardium and prevent ventricular remodelling. However it is of fundamental imortance to evaluate the molecular mechanisms underlying the short-term as well as the long-term effects of this compound on the electro-mechanical properties of diabetic myocardial tissue.

This is an important point to be explored by considering that global heart function strictly depends on the unique three-dimensional myocardial fibre architecture and the complex interplay of intrinsic mechanisms which regulate the sequential rise and fall of cytosolic Ca2+.

For this reason future studies will be focused on the evaluation of early RSV treatment on several target molecules which are involved in the excitation-contraction coupling with major attention on: 1) L-type Ca^{2+} channels responsible for Ca^{2+} entry during membrane depolarization, 2) ryanodine receptors which allow calcium-induced calcium release from the sarcoplasmic reticulum, 3) Troponin C, the protein subunit binding cytosolic Ca^{2+}, critical first step that triggers actin-myosin interaction, 4) SR Ca^{2+} ATPase (SERCA2a) as the major mechanism involved in cytosolic calcium clearing, and 5) Phospholamban and SIRT1, as key proteins regulating SERCA2 activity and expression levels. In addition, the RSV effects on Connexin-43 expression will be determined, by considering that cardiac electromechanical performance is also based on a proper intercellular communication and impulse propagation via gap-junctions [86, 87] whose spatial distribution and biophysical properties are important determinants of the conduction velocity and three-dimensional pattern of electrical activation.

Another important field that has to be explored is the bioavailability of Resveratrol which is modest, limiting the in vivo biological effect of the

compound and representing a barrier for the development of therapeutic applications. For this reason an increasing number of recent studies have aimed at designing novel resveratrol formulations to overcome its poor solubility, limited stability, high metablization and weak bioavailability.

Therefore the future for efficient resveratrol delivery lies in the development of innovative strategies able to overcome each of the physicochemical, pharmacokinetic and metabolic limitations that characterize the therapeutic use of this compound.

Bibliography

1. Bauters C, Lamblin N, Mc Fadden EP, Van Belle E, Millaire A, de Groote P. Influence of diabetes mellitus on heart failure risk and outcome. Cardiovasc Diabetol 2003; 2:1

2. Bell DS. Diabetic cardiomyopathy. A unique entity or a complication of coronary artery disease? Diabetes Care 1995; 18:708-14

3. Spector KS. Diabetic cardiomyopathy. Clin Cardiol 1998; 21:885-7

4. Rubler S, Dlugash J, Yuceoglu YZ, Kumral T, Branwood AW, Grishman A. New type of cardiomyopathy associated with diabetic glomerulosclerosis. Am J Cardiol 1972; 30(6):595–602

5. Chatham JC, Seymour AM. Cardiac carbohydrate metabolism in zucker diabetic fatty rats. Cardiovasc Res 2002; 55(1):104–112

6. Rodrigues B, Cam MC, McNeill JH. Myocardial substrate metabolism: implications for diabetic cardiomyopathy. J Mol Cell Cardiol 1995; 27(1):169–179

7. Eckel J, Reinauer H. Insulin action on glucose transport in isolated cardiac myocytes: signalling pathways and diabetes induced alterations. Biochem Soc Trans 1990; 18(6):1125–1127

8. Liedtke AJ, DeMaison L, Eggleston AM, Cohen LM, Nellis SH. Changes in substrate metabolism and effects of excess fatty acids in reperfused myocardium. Circ Res 1988; 62(3):535–542

9. Nakayama H, Morozumi T, Nanto S, Shimonagata T, Ohara T, Takano Y, Kotani J, Watanabe T, Fujita M, Nishio M, Kusuoka H, Hori M, Nagata S. Abnormal myocardial free fatty acid utilization deteriorates with morphological changes in the hypertensive heart. Jpn Circ J 2001; 65(9):783 787

10. Rodrigues B, Cam MC, McNeill JH. Metabolic disturbances in diabetic cardiomyopathy. Mol Cell Biochem 1998; 180(1–2):53–57

11. Yazaki Y, Isobe M, Takahashi W, Kitabayashi H, Nishiyama O, Sekiguchi M, Takemura T. Assessment of myocardial fatty acid metabolic abnormalities in patients with idiopathic dilated cardiomyopathy using 123I BMIPP SPECT: correlation with clinicopathological findings and clinical course. Heart 1999; 81(2):153–159

12. Abe T, Ohga Y, Tabayashi N, Kobayashi S, Sakata S, Misawa H, Tsuji T, Kohzuki H, Suga H, Taniguchi S, Takaki M. Left ventricular diastolic dysfunction in type 2 diabetes mellitus model rats. Am J Physiol Heart Circ Physiol 2002; 282(1):H138–H148

13. Malhotra A, Reich D, Nakouzi A, Sanghi V, Geenen DL, Buttrick PM. Experimental diabetes is associated with functional activation of protein kinase

c epsilon and phosphorylation of troponin i in the heart, which are prevented by angiotensin II receptor blockade. Circ Res 1997; 81(6):1027–1033

14. Takeda N, Nakamura I, Hatanaka T, Ohkubo T, Nagano M. Myocardial mechanical and myosin isoenzyme alterations in streptozotocin-diabetic rats. Jpn Heart J 1988; 29(4):455–463

15. Marra G, Cotroneo P, Pitocco D, Di Leo MA, Ruotolo V, Caputo S, Giardina B, Ghirlanda G, Santini SA. Early increase of oxidative stress and reduced antioxidant defenses in patients with uncomplicated type 1 diabetes: a case for gender difference. Diabetes Care 2002; 25:370-5

16. Penckofer S, Schwertz D, Florczak K. Oxidative stress and cardiovascular disease in type 2 diabetes: the role of antioxidants and prooxidants. J Cardiovasc Nurs 2002; 16:68-85

17. Mullarkey CJ, Edelstein D, Brownlee M. Free radical generation by early glycation products: a mechanism for accelerated atherogenesis in diabetes. Biochem Biophys Res Commun 1990; 173:932-9

18. Baynes JW. Role of oxidative stress in development of complications in diabetes. Diabetes 1991; 40:405-12

19. Williamson JR, Chang K, Frangos M, Hasan KS, Ido Y, Kawamura T, Nyengaard JR, van den Enden M, Kilo C, Tilton RG. Hyperglycemic pseudohypoxia and diabetic complications. Diabetes 1993; 42:801-13

20. Inoguchi T, Sonta T, Tsubouchi H, Etoh T, Kakimoto M, Sonoda N, Sato N, Sekiguchi N, Kobayashi K, Sumimoto H, Utsumi H, Nawata H. Protein kinase C dependent increase in reactive oxygen species (ROS) production in vascular tissues of diabetes: role of vascular NAD(P)H oxidase. J Am Soc Nephrol 2003; 14:S227-32

21. Alici B, Gümüstas MK, Ozkara H, Akkus E, Demirel G, Yencilek F, Hattat H. Apoptosis in the erectile tissues of diabetic and healthy rats. BJU Int 2000; 85:326-9

22. Cai L, Chen S, Evans T, Deng DX, Mukherjee K, Chakrabarti S. Apoptotic germ-cell death and testicular damage in experimental diabetes: prevention by endothelin antagonism. Urol Res 2000; 28:342-7

23. Fang ZY, Prins JB, Marwick TH. Diabetic cardiomyopathy: evidence, mechanisms, and therapeutic implications. Endocr Rev 2004; 25:543-67

24. Li X, Xu Z, Li S, Rozanski GJ. Redox regulation of Ito remodelling in diabetic rat heart. Am J Physiol Heart Circ Physiol 2005; 288:H1417-24

25. Kang YJ. Molecular and cellular mechanisms of cardiotoxicity. Environ Health Perspect 2001; 109 (Suppl 1):27-34

26. Tomita M, Mukae S, Geshi E, Umetsu K, Nakatani M, Katagiri T. Mitochondrial respiratory impairment in streptozotocin-induced diabetic rat heart. Jpn Circ J 1996; 60:673-82

27. Beltrami AP, Barlucchi L, Torella D, Baker M, Limana F, Chimenti S, Kasahara H, Rota M, Musso E, Urbanek K, Leri A, Kajstura J, Nadal-Ginard B, Anversa P. Adult cardiac stem cells are multipotent and support myocardial regeneration. Cell. 2003; 114:763-776

28. Madonna R, Rokosh G, De Caterina R, Bolli R. Hepatocyte growth factor/Met gene transfer in cardiac stem cells--potential for cardiac repair. Basic Res Cardiol. 2010; 105:443-452.

29. Stilli D, Lagrasta C, Berni R, Bocchi L, Savi M, Delucchi F, Graiani G, Monica M, Maestri R, Baruffi S, Rossi S, Macchi E, Musso E, Quaini F. Preservation of ventricular performance at early stages of diabetic cardiomyopathy involves changes in myocyte size, number and intercellular coupling. Basic Res Cardiol 2007; 102:488-499

30. Rota M, LeCapitaine N, Hosoda T, Boni A, De Angelis A, Padin-Iruegas ME, Esposito G, Vitale S, Urbanek K, Casarsa C, Giorgio M, Lüscher TF, Pelicci PG, Anversa P, Leri A, Kajstura J. Diabetes promotes cardiac stem cell aging and heart failure, which are prevented by deletion of the p66shc gene. Circ Res 2006; 99:42-52

31. Kajstura J, Urbanek K, Rota M, Bearzi C, Hosoda T, Bolli R, Anversa P, Leri A. Cardiac stem cells and myocardial disease. J Mol Cell Cardiol 2008; 45: 505–513

32. Pervaiz S, Taneja R, Ghaffari S. Oxidative stress regulation of stem and progenitor cells. Antioxid Redox Signal. 2009; 11:2777-2789

33. Chen Q, Dong L, Wang L, Kang L, Xu B. Advanced glycation end products impair function of late endothelial progenitor cells through effects on protein kinase Akt and cyclooxygenase-2. Biochem Biophys Res Commun 2009; 381: 192-197

34. Vastano BC, Chen Y, Zhu N, Ho CT, Zhou Z, Rosen RT. Isolation and identification of stilbenes in two varieties of Polygonum cuspidatum. J. Agric. Food Chem 2000; 48:253-256

35. Dixon RA, Paiva NL. Stress-induced phenylpropanoid metabolism. Plant Cell 1995; 7(7):1085-1097

36. Halls C, Yu O. Potential for metabolic engineering of resveratrol biosynthesis. Trends Biotechnol 2008; 26(2):77-81

37. Manach C, Williamson G, Morand C, Scalbert A, Rémésy C. Bioavaibility and bioefficacy of polyphenols in humans. I. Review of 97 bioavailability studies. Am J Clin Nutr 2005; 81:230S-242S

38. Renaud S, De Lorgeril M. Wine, alcohol, platelets, and the French paradox for coronary heart disease. Lancet 1992; 339 (8808):1523-6

39. Soleas GJ, Diamandis EP, Goldberg DMJ. Wine as a biological fluid: history, production, and role in disease prevention. J Clin Lab Anal. 1997; 11(5):287-313

40. Ignatowicz E, Baer-Dubowska W. Resveratrol, a natural chemopreventive agent against degenerative diseases. Pol J Pharmacol. 2001; 53(6):557-69

41. Petrovski G, Gurusamy N, and Das DK. Resveratrol in cardiovascular health and disease. Ann NY Acad Sci 2011; 1215:22-33

42. Camins A, Sureda FX, Junyent F, Verdaguer E, Folch J, Pelegri C, Vilaplana J, Beas-Zarate C, Pallàs M. Sirtuin activators: designing molecules to extend life span. Biochim Biophys Acta. 2010; 1799(10-12):740-9

43. Ungvari Z, Bagi Z, Feher A, Recchia FA, Sonntag WE, Pearson K, de Cabo R, Csiszar A. Resveratrol confers endothelial protection via activation of the antioxidant transcription factor Nrf2. Am J Physiol Heart Circ Physiol 2010; 299:H18-H24

44. Palsamy P, Subramanian S. Modulatory effects of resveratrol on attenuating the key enzymes activities of carbohydrate metabolism in streptozotocin-nicotinamide-induced diabetic rats. Chem Biol Interact 2009; 179:356-362

45. Zhang H, Morgan B, Potter BJ, Ma L, Dellsperger KC, Ungvari Z, Zhang C. Resveratrol Improves Left Ventricular Diastolic Relaxation in Type 2 Diabetes by Inhibiting Oxidative/Nitrative Stress: in vivo Demonstration with Magnetic Resonance Imaging. Am J Physiol Heart Circ Physiol 2010; 299:H985-H994

46. Thirunavukkarasu M, Penumathsa SV, Koneru S, Juhasz B, Zhan L, Otani H, Bagchi D, Das DK, and Maulik N. Resveratrol alleviates cardiac dysfunction in streptozotocin-induced diabetes: Role of nitric oxide, thioredoxin, and heme oxygenase. Free Radic Biol Med 2007; 43:720-729

47. Sulaiman M, Matta MJ, Sunderesan NR, Gupta MP, Periasamy M, Gupta M. Resveratrol, an activator of SIRT1, upregulates sarcoplasmic calcium ATPase and improves cardiac function in diabetic cardiomyopathy. Am J Physiol Heart Circ Physiol 2010; 298:H833-H843

48. Balestrieri ML, Schiano C, Felice F, Casamassimi A, Balestrieri A, Milone L, Servillo L, Napoli C. Effect of low doses of red wine and pure resveratrol on circulating endothelial progenitor cells. J Biochem 2008; 143:179-186

49. Gurusamy N, Ray D, Lekli I, Das DK. Red wine antioxidant resveratrol-modified cardiac stem cells regenerate infarcted myocardium. J Cell Mol Med 2010; 14:2235-2239

50. Poornima IG, Parikh P, Shannon RP. Diabetic cardiomyopathy: the search for a unifying hypothesis. Circ Res 2006; 98:596-605

51. Suurmeijer AJ, Clément S, Francesconi A, Bocchi L, Angelini A, Van Veldhuisen DJ, Spagnoli LG, Gabbiani G, Orlandi A. Alpha-actin isoform distribution in normal and failing human heart: a morphological, morphometric, and biochemical study. J Pathol 2003; 99:387-397

52. Myreng Y, Smiseth OA. Assessment of left ventricular relaxation by Doppler echocardiography. Comparison of isovolumic relaxation time and transmitral flow velocities with time constant isovolumic relaxation. Circulation 1990; 81:260-266

53. Zaniboni M, Pollard AE, Yang L, Spitzer KW. Beat-to-beat repolarization variability in ventricular myocytes and its suppression by electrical coupling. Am J Physiol Heart Circ Physiol 2000; 278:H677-H687

55. Bearzi C, Rota M, Hosoda T, Tillmanns J, Nascimbene A, De Angelis A, Yasuzawa-Amano S, Trofimova I, Siggins RW, Lecapitaine N, Cascapera S, Beltrami AP, D'Alessandro DA, Zias E, Quaini F, Urbanek K, Michler RE, Bolli R, Kajstura J, Leri A, Anversa P. Human cardiac stem cells. Proc Natl Acad Sci U S A 2007; 104:14068-14073

54. Beltrami AP, Barlucchi L, Torella D, Baker M, Limana F, Chimenti S, Kasahara H, Rota M, Musso E, Urbanek K, Leri A, Kajstura J, Nadal-Ginard B, Anversa P. Adult cardiac stem cells are multipotent and support myocardial regeneration. Cell 2003; 114:763-776

56. Dodge HT, Baxley WA. Left ventricular volume and mass and their significance in heart disease. Am J Cardiol 1969; 23:528-537

57. Berni R, Savi M, Bocchi L, Delucchi F, Musso E, Chaponnier C, Gabbiani G, Clement S, Stilli D. Modulation of actin isoform expression before the transition from experimental compensated pressure-overload cardiac hypertrophy to decompensation. Am J Physiol Heart Circ Physiol 2009; 296:H1625-H1632

58. Clément S, Stouffs M, Bettiol E, Kampf S, Krause KH, Chaponnier C, Jaconi M. Expression and function of alpha-smooth muscle actin during embryonic-stem-cell-derived cardiomyocyte differentiation. J Cell Sci 2007; 120:229-238

59. Skalli O, Ropraz P, Trzeciak A, Benzonana G, Gillessen D, Gabbiani G. A monoclonal antibody against alpha-smooth muscle actin: a new probe for smooth muscle differentiation. J Cell Biol 1986; 103:2787-2796

60. Clément S, Chaponnier C, Gabbiani G. A subpopulation of cardiomyocytes expressing alpha-skeletal actin is identified by a specific polyclonal antibody. Circ Res 1999; 85:e51-e58

61. Dugina V, Zwaenepoel I, Gabbiani G, Clément S, Chaponnier C. Beta and gamma-cytoplasmic actins display distinct distribution and functional diversity. J Cell Sci 2009; 122:2980-2988

62. Cohen BH. One-Way Independent ANOVA. In: Explaining Psychological Statistics (2nd ed.). Hoboken-NJ: John Wiley & Sons 2001, Inc. pp 324-359

63. Leri A, Kajstura J, Anversa P. Role of cardiac stem cells in cardiac pathophysiology: a paradigm shift in human myocardial biology. Circ Res 2011; 109:941-961

64. Picchi A, Capobianco S, Qiu T, Focardi M, Zou X, Cao JM, Zhang C. Coronary microvascular dysfunction in diabetes mellitus: A review. World J Cardiol 2010; 2:377-390

65. Madonna R, De Caterina R. Cellular and molecular mechanisms of vascular injury in diabetes--part II: cellular mechanisms and therapeutic targets. Vascul Pharmacol 2011; 54:75-79

66. Khullar M, Al-Shudiefat AA, Ludke A, Binepal G, Singal PK. Oxidative stress: a key contributor to diabetic cardiomyopathy. Can J Physiol Pharmacol 2010; 88:233-240

67. Shin SM, Cho IJ, Kim SG. Resveratrol protects mitochondria against oxidative stress through AMP-activated protein kinase-mediated glycogen synthase kinase-3beta inhibition downstream of poly(ADP-ribose)polymerase-LKB1 pathway. Mol Pharmacol. 2009; 76(4):884-95

68. Park DW, Baek K, Kim JR, Lee JJ, Ryu SH, Chin BR, Baek SH. Resveratrol inhibits foam cell formation via NADPH oxidase 1-mediated reactive oxygen species and monocyte chemotactic protein-1. Exp Mol Med 2009; 41:171-179

69. Mukherjee S, Lekli I, Gurusamy N, Bertelli AA, Das DK. Expression of the longevity proteins by both red and white wines and their cardioprotective components, resveratrol, tyrosol, and hydroxytyrosol. Free Radic Biol Med 2009; 46:573-578

70. Yu W, Fu YC, Zhou XH, Chen CJ, Wang X, Lin RB, Wang W. Effects of resveratrol on H(2)O(2)-induced apoptosis and expression of SIRTs in H9c2 cells. J Cell Biochem 2009; 107:741-747

71. Das M, Das DK. Resveratrol and cardiovascular health. Mol Aspects Med 2010; 31:503-512

72. Kroon PA, Iyer A, Chunduri P, Chan V, Brown L. The cardiovascular nutrapharmacology of resveratrol: pharmacokinetics, molecular mechanisms and therapeutic potential. Curr Med Chem 2010; 17:2442-2455

73. Dudley J, Das S, Mukherjee S, Das DK. Resveratrol, a unique phytoalexin present in red wine, delivers either survival signal or death signal to the ischemic myocardium depending on dose. Journal of Nutritional Biochemistry 2009; 20:443-452

74. Pasciu V, Posadino AM, Cossu A, Sanna B, Tavolini B, Gaspa L, Marchisio A, Dessole S, Capobianco G, and Pintus GF. Akt Downregulation by Flavin Oxidase–Induced ROS Generation Mediates Dose-Dependent Endothelial Cell Damage Elicited by Natural Antioxidants. Toxicological Sciences 2010; 114:101-112

75. Albiero M, Menegazzo L, Boscaro E, Agostini C, Avogaro A, Fadini GP. Defective recruitment, survival and proliferation of bone marrow-derived progenitor cells at sites of delayed diabetic wound healing in mice. Diabetologia 2011; 54:945-953

76. Westermann D, Van Linthout S, Dhayat S, Dhayat N, Escher F, Bucker-Gartner C, Spillmann F, Noutsias M, Riad A, Schultheiss HP, Tschope C. Cardioprotective and Anti-Inflammatory Effects of Interleukin Converting Enzyme Inhibition in Experimental Diabetic Cardiomyopathy. Diabetes 2007; 56:1834-1841

77. Younce CW, Kolattukudy PE. MCP-1 causes cardiomyoblast death via autophagy resulting from ER stress caused by oxidative stress generated by inducing a novel zinc-finger protein, MCPIP. Biochem J 2010; 426:43-53

78. Bustin M. Regulation of DNA-dependent activities by the functional motifs of the high-mobility-group chromosomal proteins. Mol Cell Biol.1999; 19(8):5237-46

79. Bianchi ME, Beltrame M. Upwardly mobile proteins. Workshop: the role of HMG proteins in chromatin structure, gene expression and neoplasia. EMBO Rep. 2000; 1(2):109-14

80. Scaffidi P, Mistelli T, Bianchi ME. Release of chromatin protein HMGB1 by necrotic cells triggers inflammation. Nature 2002; 418:191-195.41

81. Andersson U, Wang H, Palmblad K, Aveberger AC, Erlandsson-Harris H, Janson A, Kokkola R, Zhang M, Yang H, Tracey KJ. High Mobility group 1 protein (HMG-1) stimulates proinflammatory cytokines synthesis in human monocytes. J Exp Med 2000; 192:565-570

82. Park JS, Arcaroli J, Yum HK, Yang H, Wang H, Yang KY, Choe KH, Strassheim D, Pitts TM, Tracey KJ, Abraham E. Activation of gene expression in human neutrophils by high mobility group box 1 protein. Am J Physiol Cell Physiol 2003; 284:C870-C879

83. Hewett TE, Grupp IL, Grupp G, Robbins J. Alpha-skeletal actin is associated with increased contractility in the mouse heart. Circ Res 1994; 74:740-746

84. Vang O, Ahmad N, Baile CA, Baur JA, Brown K, Csiszar A, Das DK, Delmas D, Gottfried C, Lin HY, Ma QY, Mukhopadhyay P, Nalini N, Pezzuto JM, Richard T, Shukla Y, Surh YJ, Szekeres T, Szkudelski T, Walle T, Wu JM. What is new for an old molecule? Systematic review and recommendations on the use of resveratrol. PLoSONE 2011; 6:e19881.doi:10.1371/journal.pone.0019881

85. Amri A, Chaumeil JC, Sfar S, Charrueau C. Administration of resveratrol: What formulation solutions to bioavailability limitations? J Control Release 2011; doi:10.1016/j.jconrel.2011.09.083

86. Kanno S, Saffitz JE. The role of myocardial gap junctions in electrical conduction and arrhythmogenesis. Cardiovasc Pathol 2001; 10:169-177

87. Okruhlicova L, Tribulova N, Misejkova M, Kucka M, Stetka R, Slezak J, Manoach M. Gap junction remodelling is involved in the susceptibility of diabetic rats to hypokalemia-induced ventricular fibrillation. Acta Histochem 2002; 104:387-391

Grazie

Publications

1. Stilli D, Lagrasta C, Berni R, Bocchi L , Savi M, Delucchi F, Graiani G, Monica M, Maestri R, Baruffi S, Rossi S, Macchi E, Musso E, Quaini F. Preservation of ventricular performance at early stages of diabetic cardiomyopahty involves changes in myocyte size, number and intercellular coupling. Basic Res Cardiol., 102(6):488-499, 2007

2. Murasky JA, Rota M, Misao Y, Fransioli J, Cottage C, Fischer K, Esposito G, Delucchi F, Arcarese M, Alvarez R, Siddiqi S, Emanuel GN, Wu W, Gude N, Leri A, Kajstura J, Magnuson N, Berns A, Houser SR, Schaefer EM, Anversa P, Sussman MA. Pim-1 regulates cardiomyocyte survival downstream of AKT. Nature Medicine, 13(12):1467-75, 2007

3. Boni A, Urbanek K, Nascimbene A, Hosoda T, Zheng H, Delucchi F, Amano K, González A, Vitale S, Ojaimi C, Rizzi R, Bolli R, Yutzey K, Rota M, Kajstura J, Anversa P, Leri A. Notch1 regulates the fate of cardiac progenitor cells. Proc Natl Acad Sci USA, 105(40):15529-34, 2008

4. Berni R, Savi M, Bocchi L, Delucchi F, Musso E, Chaponnier C, Gabbiani G, Clement S, Stilli D. Modulation of actin isoform expression before the transition from experimental compensated pressure-overload cardiac hypertrophy to decompensation. Am J Physiol Heart Circ Physiol, 296(5):H1625-32, 2009

5. Colussi C, Berni R, Rosati J, Straino S, Vitale S, Spallotta F, Baruffi S, Bocchi L, Delucchi F, Rossi S, Savi M, Rotili D, Quaini F, Macchi E, Stilli D, Musso E, Mai A, Gaetano C, Capogrossi MC. The Histone deacetylase inhibitor suberoylanilide hydroxamic acid reduces cardiac arrhythmias in dystrophic mice. Cardiovasc Res. 2010 Feb 17. PMID:20164117

6. Urbanek K, Cabral-da-Silva MC, Ide-Iwata N, Maestroni S, Delucchi F, Zheng H, Ferriera-Martins J, Ogorek B, D'Amario D, Bauer M, Zerbini G, Rota M, Hosoda T, Liao R, Anversa P, Kajstura J, Leri A. Inhibition of Notch1-dependent cardiomyogenesis leads to a dilated myopathy in the neonatal heart. Circ Res. 2010 Aug 6; 107(3):429-41

7. Delucchi F, Berni R, Frati C, Cavalli S, Graiani G, Sala R, Chaponnier C, Gabbiani G, Lagrasta C, Quaini F, Stilli D. Resveratrol treatment reduces cardiac progenitor cell dysfunction and prevents morpho-functional ventricular remodeling in type-1 diabetic rats. PLoS One. 2012; Submitted